


Two-fluid kinetic theory for dilute polymer solutionsShiwani Singh ^{1,2,*}, Ganesh Subramanian,^{2,†} and Santosh Ansumali^{2,‡}¹*Mathematics Institute, University of Warwick, Coventry CV4 7AL, United Kingdom*²*Engineering Mechanics Unit, JNCASR, Jakkur, Bangalore 560064, India*

(Received 26 January 2022; accepted 7 September 2022; published 3 October 2022)

We provide a Boltzmann-type kinetic description for dilute polymer solutions based on two-fluid theory. This Boltzmann-type description uses a quasiequilibrium based relaxation mechanism to model collisions between a polymer dumbbell and a solvent molecule. The model reproduces the desired macroscopic equations for the polymer-solvent mixture. The proposed kinetic scheme leads to a numerical algorithm which is along the lines of the lattice Boltzmann method. Finally, the algorithm is applied to describe the evolution of a perturbed Kolmogorov flow profile, whereby we recover the major elastic effect exhibited by a polymer solution, specifically, the suppression of the original inertial instability.

DOI: [10.1103/PhysRevE.106.044501](https://doi.org/10.1103/PhysRevE.106.044501)**I. INTRODUCTION**

The numerical modeling of flows of polymeric liquids is often done via micro-macro simulations where one couples a continuum Navier-Stokes solver with a microscopic solver for the polymer dynamics. One of the simplest micromechanical approaches for modeling dilute polymer solutions in this manner is to treat them as a suspension of noninteracting elastic dumbbells immersed in a Newtonian solvent [1,2]. For Hookean dumbbells, it is also possible to obtain a macroscopic constitutive equation for the stress tensor in closed form (the Oldroyd-B model [1–3]), and thereby, have a purely continuum model for flow behavior. The distinct advantage of using a microscopic approach for the polymer is that it is possible to solve for the flow even in circumstances which preclude the derivation of a closed-form constitutive equation in terms of macroscopic variables. The latter is the case for a suspension of FENE (finitely extensible nonlinearly elastic) dumbbells [4–6]. In most of the micro-macro approaches, the macroscopic flow solver, which solves the equations of motion using standard numerical techniques (finite difference or finite element), is coupled with microscopic Brownian dynamics (BD) simulations where one solves a large system of Langevin equations for the actual polymer molecules (the so-called CONFESSIT approach), or equivalent Brownian configuration fields, to obtain ensemble-averaged configuration statistics [7–10]. Thus, in this approach, while the kinetic theory of polymer dynamics, based on an underlying Fokker-Planck equation, is considered, the solvent is still treated at the continuum level. In recent years, kinetic-theory-based solvers such as the lattice Boltzmann (LB) formulation have emerged as an alternative to direct solvers of Navier-Stokes equations [11–13]. Due to the efficiency of such solvers, instead of

micro-macro coupling, meso-micro coupling, wherein mesoscopic solvent flow solvers [LB, dissipative particle dynamics (DPD), or multiparticle collision dynamics (MPCD)] replace the macroscopic flow solvers, is increasingly being advocated [14–18]. In many of these cases, the polymer-solvent coupling is achieved by a simple dissipative ansatz [14,17]. It would be natural to provide a kinetic theory framework where, along the lines of the original and classical case of gaseous mixtures [19,20], the solvent and solute are both modeled at the mesoscopic level. In the present case, this would imply a Boltzmann (or BGK)-based description of the solvent and a Fokker-Planck-type description of the polymer, and the aforementioned dissipative coupling would then emerge naturally in the resulting moment equations. A number of discrete algorithms exist where some version of polymer kinetic or constitutive equation is solved along with an LB solver for the fluid [21–23]. To the best of our knowledge, however, a Boltzmann- (or Fokker-Planck-) type kinetic formulation, which can describe the two-fluid dynamics of a polymer-solvent mixture, does not exist.

Moreover, any attempt to extend the original Boltzmann mixture theory has to consider fundamental issues absent in the kinetic theories for mixtures of structureless particles [19,20]. For example, modeling the polymer-solvent mixture needs one to account for the internal microstructure of the polymer molecules. It is the existence of these internal configurational degrees of freedom that lead to the characteristic entropic elasticity associated with flexible polymer chains. The momentum balance for a polymer solution may be written in the form [24]:

$$\frac{\partial \mathbf{J}}{\partial t} + \frac{\partial}{\partial \mathbf{r}}(\rho \mathbf{U} \mathbf{U}) = -\frac{\partial}{\partial \mathbf{r}}(p + P_p^{\text{osmotic}}) + \frac{\partial}{\partial \mathbf{r}} \cdot (\mathbf{\Pi}_S + \mathbf{\Pi}_P), \quad (1)$$

where ρ is the total density, \mathbf{J} is the total momentum density, p the hydrodynamic pressure, $\mathbf{\Pi}_S = \eta_s[\nabla \mathbf{u}_S + (\nabla \mathbf{u}_S)^T]$ is the Newtonian viscous stress tensor with η_s being the solvent viscosity, P_p^{osmotic} is the additional osmotic stress due to the

* shiwani.singh@warwick.ac.uk

† sganesh@jncasr.ac.in

‡ ansumali@jncasr.ac.in

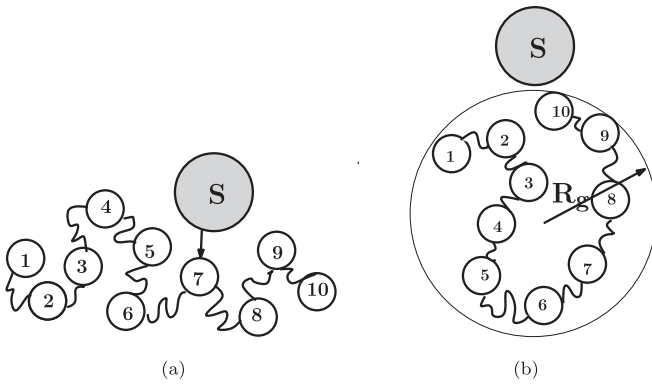


FIG. 1. Collision mechanisms. (a) Bead-centered collision. (b) Collision with effective sphere, R_g being the radius of gyration.

suspended polymer molecules, and Π_P is the polymeric elastic stress tensor arising due to the nonlocal nature of momentum transport via the polymeric back-bone, and as mentioned above, reliant on internal degrees of freedom for its existence. The different stress contributions in the momentum balance above are well understood in terms of their relative importance [1]. The formulation of a phase-space kinetic theory for a polymer-solvent mixture raises the immediate question as to how to model the emergence of a nonlocal polymeric stress from the local collision picture of Boltzmann kinetic theory. Unlike the case of a simple gas mixture, such a nonlocal contribution emerges from describing the polymeric solute (modeled as a bead-spring chain with N beads, say) in terms of an N -particle distribution function. Thus, any detailed kinetic model of a polymeric solution needs to couple the N -particle kinetic theory of the solute (the precise value of N being dictated by the micromechanical model used; $N = 2$ for a dumbbell) with the single-particle kinetic theory of the solvent. Such a scenario requires new ingredients to be incorporated in a Boltzmann-type kinetic theory for mixtures of simple gases. For example, what does one mean by a collisional event? Does one speak of a collision between a bead and solvent or one between an effective sphere formed by the chain and the solvent molecule (see Fig. 1). What are the collisional invariants and set of slow moments in such a kinetic theory? Further, it is not obvious *a priori* if, starting from a nonlocal description of a polymer dumbbell, the local collision inherent in Boltzmann kinetic theory can provide a set of slow moments defined in a pointwise manner. Finally and importantly, how does the well known entropic polymeric stress arise in this kinetic description?

In the rheological context, the characteristic timescales of interest ensure that the polymer concentration is almost always regarded as uniform. This is reflected in the vast majority of macroscopic constitutive equations in polymer rheology being derived based only on the (internal) conformational degrees of freedom of the polymer molecules. The positional degrees of freedom are irrelevant owing to the small center-of-mass diffusivities of the suspended macromolecules, and the resulting long timescales that typically characterize the development of concentration inhomogeneities. There are at least two exceptions to this rule. The first is the dynamics of polymer-solvent mixtures close to the critical point

where the enhanced osmotic compressibility renders concentration fluctuations important. It is known that elastic stresses associated with the dynamics of the inhomogeneous polymer concentration field, when coupled to an ambient shear flow, lead to enhanced scattering in the single phase region above the critical point [25,26]. In attempting to model these concentration fluctuations, which differ qualitatively from those of simple fluid mixtures close to the critical point, researchers have used two-fluid equations at the continuum level [24,27–30]. In these models, the independent variables of interest are the polymer and solvent mass and momentum densities. The component mass densities satisfy the respective continuity equations. The momentum balance for the Newtonian solvent involves the familiar viscous stress, while the polymer is also acted on by a combination of osmotic and elastic stresses that are nontrivial functions of the polymer concentration. Such a coupling mechanism between the polymer stresses and concentration, as proposed in Ref. [27], has often been used to explain the shear banding in polymer solutions and other complex fluids [31,32]. In addition, each of these species is acted on by an interphase drag force that resists any relative motion. The second scenario where the inhomogeneity of the polymer concentration field becomes important is in shearing flows of polymer solutions in confined geometries, specifically microfluidic channels [33]. In these cases, the polymer residence time becomes long enough to be comparable to the timescale of stress-driven migration in the transverse direction; essentially on account of the disparity between the longitudinal and transverse channel dimensions. There have been several attempts to explain the phenomenon of stress-driven migration that leads to concentration inhomogeneities manifesting as near-wall depletion layers [34–37]. Some of these efforts again are kinetic-theory-based with the solvent still treated as a continuum [38,39], while others employ a more formal approach based on the Hamiltonian theory of nonequilibrium thermodynamics [40,41]. A third scenario where the diffusive degrees of freedom of the suspended microstructure are of importance is shear-banding instabilities that are known to occur in wormlike micellar solutions [32].

Keeping in mind the aforementioned earlier approaches to the dynamics and rheology of polymer solutions, the two-component phase-space kinetic theory for polymer solutions formulated in this paper leads to a computationally efficient numerical algorithm that allows for the (1) the characterization of complex flows, both nonviscometric laminar and turbulent, of polymer solutions free of closure approximations that characterize earlier macroscopic constitutive-equation-based approaches (for instance, see [42,43]); (2) prediction of near-critical dynamics of polymer molecules without the approximation underlying earlier phenomenological descriptions; and (3) prediction of stress-driven migration of polymer molecules in confined geometries, and the associated characterization of wall-depletion layers.

The paper is organized as follows. A brief description of the Boltzmann-based kinetic theory of a binary (simple) gas mixture is given in Sec. II. Then in Sec. III we describe the kinetic-theory-based approach for a polymer solvent mixture, wherein the polymer is modeled as a dumbbell and the solvent molecules are structureless particles, and the moment equations for which are consistent with the phenomenological

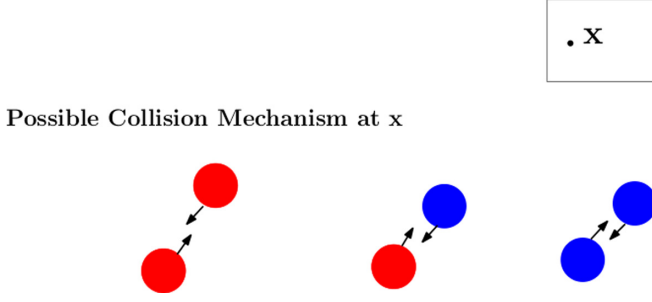


FIG. 2. Schematic showing different types of collision in a binary gas mixture.

description used in the analysis of concentration fluctuations in near-critical polymer solutions. In Sec. IV the collision model for a binary gas mixture required within the framework of a numerical implementation, is discussed. The drawback of the single relaxation time approximation of the BGK collision model is pointed out to begin with, which is that of having a fixed Schmidt (Sc) number. This is followed by the introduction of quasiequilibrium-based collision models with a tunable Schmidt number. Section V deals with a quasiequilibrium-based collision model for a polymer-solvent mixture, which is shown to reproduce the desired continuum description. The discrete numerical scheme is discussed in Sec. VI where, starting with the description of the popular two dimensional lattice model for solvent in Sec. VIA, we introduce the unconventional hyper-lattice model to solve for the two-particle distribution function of polymer dumbbell in Sec. VIB. This is followed by a review of the time discretization scheme, and the boundary conditions in the discrete orientation space, in Sec. VIC. In Sec. VII the effect of polymers in the suppression of inertial instabilities is illustrated for the specific case of a Kolmogorov flow. Finally, the work is summarized in Sec. VIII.

II. THE BOLTZMANN EQUATION FOR A BINARY MIXTURE

In this section, we briefly recall the Boltzmann model as applied to a binary gas mixture [44,45]. In a binary gas mixture consisting of two components with masses m_j ($j = A, B$), in addition to the self-collisions of the A and B particles, cross-collisions between the A and B particles also occur. Thus, as shown in Fig. 2, three kinds of collisions can occur at a given spatial location \mathbf{x} at any instant in time. The kinetic equations governing the evolution of the probability distribution functions of the individual components ($f_A(\mathbf{x}, \mathbf{v}_A, t)$ and $f_B(\mathbf{x}, \mathbf{v}_B, t)$) are

$$\begin{aligned} \frac{\partial}{\partial t} f_A(\mathbf{x}, \mathbf{v}_A, t) + \mathbf{v}_A \cdot \frac{\partial f_A}{\partial \mathbf{x}} &= \underbrace{\Omega_{AA}(f_A, f_A) + \Omega_{AB}(f_A, f_B)}_{\Omega_A}, \\ \frac{\partial}{\partial t} f_B(\mathbf{x}, \mathbf{v}_B, t) + \mathbf{v}_B \cdot \frac{\partial f_B}{\partial \mathbf{x}} &= \underbrace{\Omega_{BA}(f_B, f_A) + \Omega_{BB}(f_B, f_B)}_{\Omega_B}, \end{aligned} \quad (2)$$

where $f_j(\mathbf{x}, \mathbf{v}_j, t)$ denotes the probability density of finding a molecule of component j ($j = A$ or B) at position \mathbf{x} and time

t . Ω_{AA} , Ω_{BB} are the self-collision contributions and Ω_{AB}/Ω_{BA} is the cross-collision contribution which is expressed as [46]

$$\begin{aligned} \Omega_{jk}(f_j, f_k) &= \int d\mathbf{v}'_j d\mathbf{v}'_k d\mathbf{v}_k [f_j(\mathbf{x}, \mathbf{v}'_j, t) f_k(\mathbf{x}, \mathbf{v}'_k, t) \\ &\quad - f_j(\mathbf{x}, \mathbf{v}_j, t) f_k(\mathbf{x}, \mathbf{v}_k, t)] \omega(\mathbf{v}'_j, \mathbf{v}'_k | \mathbf{v}_j, \mathbf{v}_k). \end{aligned} \quad (3)$$

The transition probability density, $\omega(\mathbf{v}'_j, \mathbf{v}'_k | \mathbf{v}_j, \mathbf{v}_k)$ in Eq. (3), defines the probability that a binary collision between molecules of the components j and k at a given location \mathbf{x} , with velocities \mathbf{v}_j and \mathbf{v}_k , leads to velocities \mathbf{v}'_j and \mathbf{v}'_k in accordance with the laws of an elastic collision:

$$\begin{aligned} m_j \mathbf{v}_j + m_k \mathbf{v}_k &= m_j \mathbf{v}'_j + m_k \mathbf{v}'_k, \\ m_j v_j^2 + m_k v_k^2 &= m_j v_j'^2 + m_k v_k'^2. \end{aligned} \quad (4)$$

The transition probability, ω , is symmetric with respect to its dependence on the pre- and postcollisional velocities,

$$\omega(\mathbf{v}'_j, \mathbf{v}'_k | \mathbf{v}_j, \mathbf{v}_k) = \omega(\mathbf{v}_j, \mathbf{v}_k | \mathbf{v}'_j, \mathbf{v}'_k), \quad (5)$$

reflecting the detailed balance that exists at equilibrium. Self-collisions do not affect mass, momentum and energy conservation. Cross-collisions too do not affect the mass conservation, and one obtains the usual continuity equations for the individual components. However, momentum and kinetic energy are exchanged between components via cross-collisions in such a manner that the total momentum and energy are conserved.

Using the kinetic equations (2), the evolution equations for the component momenta, defined by $\mathbf{J}_j = \langle m_j \mathbf{v}_j, f_j \rangle$, are given by [46]

$$\begin{aligned} \frac{\partial \mathbf{J}_A}{\partial t} + \frac{\partial}{\partial \mathbf{x}} \cdot \mathbf{P}_A &= \langle \Omega_{AB}, m_A \mathbf{v}_A \rangle, \\ \frac{\partial \mathbf{J}_B}{\partial t} + \frac{\partial}{\partial \mathbf{x}} \cdot \mathbf{P}_B &= \langle \Omega_{BA}, m_B \mathbf{v}_B \rangle, \end{aligned} \quad (6)$$

where the component momentum fluxes (or stress tensors) are defined by $\mathbf{P}_j = \langle m_j \mathbf{v}_j \mathbf{v}_j, f_j \rangle$ in the above equations, and the angular brackets denote a velocity-space average with respect to f_j , so $\langle \phi, f_j \rangle = \int f_j \phi d\mathbf{v}_j$. Using (3), we get

$$\begin{aligned} \langle \Omega_{AB}, m_A \mathbf{v}_A \rangle &= m_A \int d\mathbf{v}_A d\mathbf{v}'_A d\mathbf{v}_B d\mathbf{v}'_B (\mathbf{v}'_A - \mathbf{v}_A) \\ &\quad \times f_A(\mathbf{x}, \mathbf{v}'_A, t) f_B(\mathbf{x}, \mathbf{v}'_B, t) \omega, \\ \langle \Omega_{BA}, m_B \mathbf{v}_B \rangle &= m_B \int d\mathbf{v}_A d\mathbf{v}'_A d\mathbf{v}_B d\mathbf{v}'_B (\mathbf{v}'_B - \mathbf{v}_B) \\ &\quad \times f_A(\mathbf{x}, \mathbf{v}'_A, t) f_B(\mathbf{x}, \mathbf{v}'_B, t) \omega. \end{aligned} \quad (7)$$

Using momentum conservation given by (4), in (7), we get

$$\langle \Omega_{AB}, m_A \mathbf{v}_A \rangle + \langle \Omega_{BA}, m_B \mathbf{v}_B \rangle = 0. \quad (8)$$

Thus, the cross-collisions between the two species are solely responsible for momentum exchange, and the corresponding

flux can be defined as

$$\mathbf{V}_D = \frac{\tau_{AB}}{2} (\langle \Omega_{AB}, m_A \mathbf{v}_A \rangle - \langle \Omega_{BA}, m_B \mathbf{v}_B \rangle), \quad (9)$$

where \mathbf{V}_D is the diffusion flux that characterizes the aforementioned exchange process, and the associated timescale τ_{AB} is the mean free time which can be extracted from the cross-collision contribution Ω_{AB} (or Ω_{BA}). The equations for the component momenta, in terms of diffusion flux, then take the form

$$\begin{aligned} \frac{\partial \mathbf{J}_A}{\partial t} + \frac{\partial}{\partial \mathbf{x}} \cdot \mathbf{P}_A &= \frac{\mathbf{V}_D}{\tau_{AB}}, \\ \frac{\partial \mathbf{J}_B}{\partial t} + \frac{\partial}{\partial \mathbf{x}} \cdot \mathbf{P}_B &= -\frac{\mathbf{V}_D}{\tau_{AB}}. \end{aligned} \quad (10)$$

By subtracting one equation from another in Eq. (10) and using Chapman-Enskog expansion, the Stefan-Maxwell binary diffusion equations can be recovered which relate τ_{AB} and the diffusion coefficient, D_{AB} , as $D_{AB} = (X_A X_B / m_{AB}) \tau_{AB} P$, where $X_j (n_j / n)$ is the individual component mole fraction, $P (= nk_B T)$ is the thermodynamic pressure of the system and $m_{AB} [= \rho_A \rho_B / (\rho_A + \rho_B)]$ is the reduced mass with $\rho_j = \langle m_j, f_j \rangle$ [44,45]. The formal expression for the diffusion flux is provided in Sec. IV where collision models for the binary gas mixtures are discussed in detail. From the relations governing \mathbf{J}_A and \mathbf{J}_B [Eq. (10)], and with $\mathbf{J} = \mathbf{J}_A + \mathbf{J}_B$, one obtains

$$\frac{\partial \mathbf{J}}{\partial t} + \frac{\partial}{\partial \mathbf{x}} \cdot \mathbf{P} = 0, \quad (11)$$

with $\mathbf{P} = \mathbf{P}_A + \mathbf{P}_B$ which is consistent with the total mixture momentum being conserved. Similarly, the evolution of the component stress tensors is governed by equations of the form

$$\frac{\partial}{\partial t} \mathbf{P}_j + \frac{\partial}{\partial \mathbf{x}} \cdot \mathbf{Z}_j = \langle \Omega_{jj}, m_j \mathbf{v}_j \mathbf{v}_j \rangle + \langle \Omega_{jk}, m_j \mathbf{v}_j \mathbf{v}_j \rangle, \quad (12)$$

where $j \neq k$, and \mathbf{Z}_j is a third-order tensor which represents the flux corresponding to \mathbf{P}_j , and can be written in terms of the distribution function as $\mathbf{Z}_j = \langle m_j \mathbf{v}_j \mathbf{v}_j \mathbf{v}_j, f_j \rangle$. The trace of Eq. (12) for $j = A, B$ corresponds to the evolution of the component kinetic energies. Energy conservation per collision, as stated in Eq. (4), implies that the total kinetic energy is conserved [that is, $\text{tr}(\mathbf{P})$ is a constant].

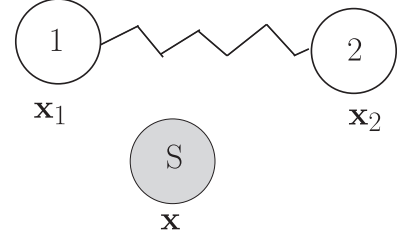


FIG. 3. Schematic showing the polymer modeled as a dumbbell and solvent as a structureless particle.

The kinetic level description of the Boltzmann type for a binary mixture, as well as the resulting low-order moment equations have been presented above. Here interactions between the molecules of the two components via cross-collisions allow for the exchange of both momentum and kinetic energy, while respecting conservation of the total momentum and kinetic energy. In the next section, based on these considerations, a more elaborate Boltzmann-type description for a polymer-solvent mixture is presented.

III. EXTENDED BOLTZMANN MIXTURE EQUATION FOR A POLYMER SOLUTION

The simplest micromechanical theory of the polymer solution is based on a two-component mixture with one of the components being a structureless solvent particle of mass m_S and the other component being a polymer dumbbell consisting of two point masses (each of mass m_B) connected by a massless spring; a schematic of the model appears in Fig. 3. The spring force is a function of the relative separation of the pair of masses, being given by $\mathbf{F}_\nu (\mathbf{x}_\xi - \mathbf{x}_\nu)$ (for $\nu, \xi = 1, 2$) such that $\mathbf{F}_1 = -\mathbf{F}_2$. Based on the schematic of the model shown in Fig. 3, we extend the Boltzmann paradigm summarized in Sec. II to the case of a dilute polymer solution.

As before, the dynamics of the solvent phase is governed by the single-particle distribution function $f_S^I(\mathbf{x}, \mathbf{v}_S, t)$ which denotes the probability of finding a solvent molecule at position \mathbf{x} with velocity \mathbf{v}_S at time t . The subscripts S, P denote solvent and polymer, respectively; note the added superscript I which helps draw a distinction to the pair probability that is relevant to the polymeric dumbbell and does not appear in the description of the simple gas mixture above. The solvent mass density ρ_S , momentum density $\rho_S \mathbf{u}_S$, and temperature T_S are defined as

$$\rho_S = \langle m_S, f_S^I \rangle, \quad \mathbf{J}_S = \rho_S \mathbf{u}_S = \langle m_S \mathbf{v}_S, f_S^I \rangle, \quad \rho_S T_S = \langle m_S (v_S - u_S)^2, f_S^I \rangle. \quad (13)$$

The dynamics of the solute (polymer modeled as a dumbbell) is governed by a two-particle distribution function $f_P^{II}(\mathbf{x}_1, \mathbf{x}_2, \mathbf{v}_{P1}, \mathbf{v}_{P2}, t)$ which defines the probability of finding the dumbbell such that the bead 1 is at \mathbf{x}_1 with velocity \mathbf{v}_{P1} and bead 2 is located at \mathbf{x}_2 with velocity \mathbf{v}_{P2} at any instant of time t . The mass density of the polymer component at the position \mathbf{x} is then defined as

$$\rho_P(\mathbf{x}, t) = m_B \int f_P^{II}(\mathbf{x}_1, \mathbf{x}_2, \mathbf{v}_{P1}, \mathbf{v}_{P2}, t) \delta(\mathbf{x} - \mathbf{x}_1) d\mathbf{v}_{P1} d\mathbf{v}_{P2} d\mathbf{x}_1 d\mathbf{x}_2 + m_B \int f_P^{II}(\mathbf{x}_1, \mathbf{x}_2, \mathbf{v}_{P1}, \mathbf{v}_{P2}, t) \delta(\mathbf{x} - \mathbf{x}_2) d\mathbf{v}_{P1} d\mathbf{v}_{P2} d\mathbf{x}_1 d\mathbf{x}_2, \quad (14)$$

which accounts for contributions of both beads. Therefore, $\rho_P = 2m_B n_P$, where n_P is the number density of polymers. Along the same lines, it is natural to define the momentum density and the stress tensor as [47]

$$\begin{aligned} \mathbf{J}_P(\mathbf{x}, t) &= m_B \int \mathbf{v}_{P1} f_P^{\text{II}}(\mathbf{x}_1, \mathbf{x}_2, \mathbf{v}_{P1}, \mathbf{v}_{P2}, t) \delta(\mathbf{x} - \mathbf{x}_1) d\mathbf{v}_{P1} d\mathbf{v}_{P2} d\mathbf{x}_1 d\mathbf{x}_2 \\ &\quad + m_B \int \mathbf{v}_{P2} f_P^{\text{II}}(\mathbf{x}_1, \mathbf{x}_2, \mathbf{v}_{P1}, \mathbf{v}_{P2}, t) \delta(\mathbf{x} - \mathbf{x}_2) d\mathbf{v}_{P1} d\mathbf{v}_{P2} d\mathbf{x}_1 d\mathbf{x}_2, \end{aligned} \quad (15)$$

$$\begin{aligned} \mathbf{P}_P(\mathbf{x}, t) &= m_B \int \mathbf{v}_{P1} \mathbf{v}_{P1} f_P^{\text{II}}(\mathbf{x}_1, \mathbf{x}_2, \mathbf{v}_{P1}, \mathbf{v}_{P2}, t) \delta(\mathbf{x} - \mathbf{x}_1) d\mathbf{v}_{P1} d\mathbf{v}_{P2} d\mathbf{x}_1 d\mathbf{x}_2 \\ &\quad + m_B \int \mathbf{v}_{P2} \mathbf{v}_{P2} f_P^{\text{II}}(\mathbf{x}_1, \mathbf{x}_2, \mathbf{v}_{P1}, \mathbf{v}_{P2}, t) \delta(\mathbf{x} - \mathbf{x}_2) d\mathbf{v}_{P1} d\mathbf{v}_{P2} d\mathbf{x}_1 d\mathbf{x}_2. \end{aligned} \quad (16)$$

The stress, \mathbf{P}_P in Eq. (16) constitutes only the kinetic contribution to the stress tensor, resulting from the (ballistic) motion of the beads across a surface. The entropic stress arising due to the interparticle force is discussed later in this section. The trace of \mathbf{P}_P would be the sum of the averaged kinetic energies of the two beads which constitute a part of the osmotic pressure. The total osmotic pressure would be the sum of the kinetic energies of the two beads (compressive) and the trace of the entropic stress (tensile), this sum being proportional to the number density of dumbbells. Further, as implicit in the definitions above, a solvent-bead collision at the location of interest can involving either of the two beads. The momentum balance for each of these collisions may be written as

$$m_S \mathbf{v}_S + m_B \mathbf{v}_{P1} = m_S \mathbf{v}'_{S1} + m_B \mathbf{v}'_{P1} \quad (17)$$

and

$$m_S \mathbf{v}_S + m_B \mathbf{v}_{P2} = m_S \mathbf{v}'_{S2} + m_B \mathbf{v}'_{P2}. \quad (18)$$

The elementary collisions involved in the polymer solution are more complicated owing to the internal degree of freedom associated with the polymer molecule (dumbbell). Unlike the binary gas mixture in Sec. II, binary cross-collisions are now nonlocal. Therefore, the polymer dumbbell will collide with the solvent molecule located at \mathbf{x} if either of its beads is located at \mathbf{x} with the other bead separated by a finite distance \mathbf{Q} (see Fig. 4). Here it should be pointed out that the kinetic description of the polymer solution simplifies in terms of a one particle probability distribution defined as

$$\begin{aligned} f_P^1(\mathbf{x}, \mathbf{v}_P, t) &= \int d\mathbf{x}_2 d\mathbf{v}_{P2} f_P^{\text{II}}(\mathbf{x}, \mathbf{x}_2, \mathbf{v}_P, \mathbf{v}_{P2}, t) \\ &\quad + \int d\mathbf{x}_1 d\mathbf{v}_{P1} f_P^{\text{II}}(\mathbf{x}_1, \mathbf{x}, \mathbf{v}_{P1}, \mathbf{v}_P, t), \end{aligned} \quad (19)$$

which corresponds to the probability of finding either of the beads of the dumbbell at \mathbf{x} with velocity \mathbf{v}_P . Before we intro-

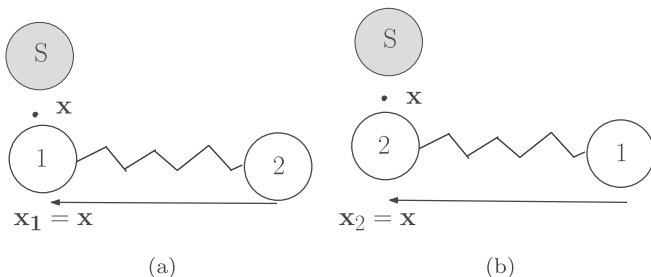


FIG. 4. Possible cross-collision between solvent molecule and polymer dumbbell at location \mathbf{x} . (a) Possibility 1 (b) Possibility 2.

duce the simplified form of the kinetic equations, we present another way of representing the dumbbell configuration space which is shown in Fig. 5, where the configuration of a polymer dumbbell is defined in terms of \mathbf{r} and \mathbf{Q} with $\mathbf{Q} = \mathbf{x}_2 - \mathbf{x}_1$. This corresponds to either bead 1 or 2 being at location \mathbf{r} (the other being at $\mathbf{r} \pm \mathbf{Q}$), with velocity \mathbf{v}_P . The velocity of the end-to-end vector \mathbf{Q} is denoted as $\dot{\mathbf{Q}}$. The center of mass, in this notation, is located at $\mathbf{r} - \mathbf{R}_v$, where $\mathbf{R}_v = (-1)^v \mathbf{Q}/2$ is the vector from the center of mass of the dumbbell to the v^{th} bead; the velocity associated with the center of mass being $\mathbf{v}_P - \dot{\mathbf{R}}_v$. This (\mathbf{r}, \mathbf{Q}) coordinate system will eventually be used in our kinetic modeling. The one-particle distribution function for the polymer, as defined by Eq. (19), takes the following form in $\mathbf{r} - \mathbf{Q}$ coordinates:

$$f_P^1(\mathbf{r}, \mathbf{v}_P, t) = \sum_v \int f_P^{\text{II}}(\mathbf{r} - \mathbf{R}_v, \mathbf{Q}, \mathbf{v}_P - \dot{\mathbf{R}}_v, \dot{\mathbf{Q}}, t) d\mathbf{Q} d\dot{\mathbf{Q}}. \quad (20)$$

Having clarified the basic elements involved in the probabilistic description, we now extend the kinetic model of the binary mixture in Sec. II to the case of a polymer solution using the collision picture given in Fig. 4. The model given below describes the dynamics of the solvent molecules using the one-particle distribution function $f_S^1(\mathbf{x}, \mathbf{v}_S, t)$ and that of the polymer dumbbells using the two-particle distribution function $f_P^{\text{II}}(\mathbf{x}_1, \mathbf{x}_2, \mathbf{v}_{P1}, \mathbf{v}_{P2}, t)$, and in addition, accounts for the nonlocal collision picture in Fig. 4.

The evolution equation for the solvent probability density, in a manner similar to the simple gas model given in the previous section, can be written as

$$\left(\frac{\partial}{\partial t} + \mathbf{v}_S \frac{\partial}{\partial \mathbf{x}} \right) f_S^1(\mathbf{x}, \mathbf{v}_S, t) = \Omega_{SS}(f_S^1, f_S^1) + \Omega_{SP}(f_S^1, f_P^{\text{II}}), \quad (21)$$

where Ω_{SS} accounts for the collisions between the solvent molecules, and has a form analogous to the collision terms in

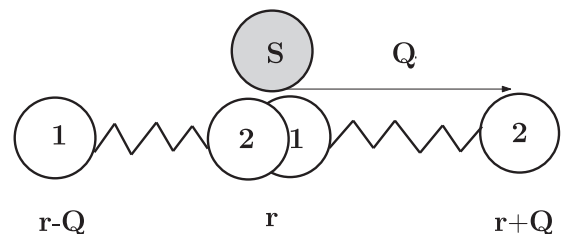


FIG. 5. Schematic of polymer configuration.

Sec. II. Ω_{SP} accounts for the cross-collision between a solvent molecule and a polymer dumbbell, and in explicit form, is given by

$$\begin{aligned} \Omega_{\text{SP}}(f_{\text{S}}^{\text{I}}, f_{\text{P}}^{\text{II}}) = & \int d\mathbf{v}'_{\text{S}1} d\mathbf{v}_{\text{P}1} d\mathbf{v}'_{\text{P}1} d\mathbf{v}'_{\text{P}2} d\mathbf{x}_2 [f_{\text{S}}^{\text{I}}(\mathbf{x}, \mathbf{v}'_{\text{S}1}, t) f_{\text{P}}^{\text{II}}(\mathbf{x}, \mathbf{x}_2, \mathbf{v}'_{\text{P}1}, \mathbf{v}'_{\text{P}2}, t) - f_{\text{S}}^{\text{I}}(\mathbf{x}, \mathbf{v}_{\text{S}}, t) f_{\text{P}}^{\text{II}}(\mathbf{x}, \mathbf{x}_2, \mathbf{v}_{\text{P}1}, \mathbf{v}_{\text{P}2}, t)] \omega_1 \\ & + \int d\mathbf{v}'_{\text{S}2} d\mathbf{v}_{\text{P}2} d\mathbf{v}'_{\text{P}2} d\mathbf{v}'_{\text{P}1} d\mathbf{x}_1 [f_{\text{S}}^{\text{I}}(\mathbf{x}, \mathbf{v}'_{\text{S}2}, t) f_{\text{P}}^{\text{II}}(\mathbf{x}_1, \mathbf{x}, \mathbf{v}'_{\text{P}1}, \mathbf{v}'_{\text{P}2}, t) - f_{\text{S}}^{\text{I}}(\mathbf{x}, \mathbf{v}_{\text{S}}, t) f_{\text{P}}^{\text{II}}(\mathbf{x}_1, \mathbf{x}, \mathbf{v}_{\text{P}1}, \mathbf{v}_{\text{P}2}, t)] \omega_2, \end{aligned} \quad (22)$$

where the short-hand notations

$$\omega_1 \equiv \omega(\mathbf{v}'_{\text{S}1}, \mathbf{v}'_{\text{P}1} | \mathbf{v}_{\text{S}}, \mathbf{v}_{\text{P}1}), \quad \omega_2 \equiv \omega(\mathbf{v}'_{\text{S}2}, \mathbf{v}'_{\text{P}2} | \mathbf{v}_{\text{S}}, \mathbf{v}_{\text{P}2}) \quad (23)$$

are used for the transition probabilities. The first integral on the right-hand side of Eq. (22) accounts for both the direct and inverse collisions between a solvent molecule and the first bead of the dumbbell. The solvent molecule moving with velocity \mathbf{v}_{S} collides with the first bead moving with velocity $\mathbf{v}_{\text{P}1}$, and located at \mathbf{x} , with both switching to postcollisional velocities $\mathbf{v}'_{\text{S}1}$ and $\mathbf{v}'_{\text{P}1}$ with probability ω_1 . Conversely, a solvent molecule with precollisional velocity $\mathbf{v}'_{\text{S}1}$ can collide with the first bead of the polymer with velocity $\mathbf{v}'_{\text{P}1}$, leading to velocities \mathbf{v}_{S} and $\mathbf{v}_{\text{P}1}$. Similarly, the second integral term accounts for the collision between solvent and the second bead of the polymer dumbbell. In terms of the reduced single-particle distribution f_{P}^{I} [see Eq. (19)], the cross-collision term in Eq. (22) may be rewritten as

$$\Omega_{\text{SP}}(f_{\text{S}}^{\text{I}}, f_{\text{P}}^{\text{I}}) = \int d\mathbf{v}'_{\text{S}} d\mathbf{v}_{\text{P}} d\mathbf{v}'_{\text{P}} [f_{\text{S}}^{\text{I}}(\mathbf{x}, \mathbf{v}'_{\text{S}}, t) f_{\text{P}}^{\text{I}}(\mathbf{x}, \mathbf{v}'_{\text{P}}, t) - f_{\text{S}}^{\text{I}}(\mathbf{x}, \mathbf{v}_{\text{S}}, t) f_{\text{P}}^{\text{I}}(\mathbf{x}, \mathbf{v}_{\text{P}}, t)] \omega_1, \quad (24)$$

which is now analogous to the cross-collision term in the Boltzmann equation for the simple gas mixture as given in Eq. (3) [48]. Similarly, the kinetic equation for the evolution of the pair-probability characterizing the polymer solute is

$$\left(\frac{\partial}{\partial t} + \mathbf{v}_{\text{P}1} \frac{\partial}{\partial \mathbf{x}_1} + \mathbf{v}_{\text{P}2} \frac{\partial}{\partial \mathbf{x}_2} + \frac{\mathbf{F}_1}{m_{\text{B}}} \frac{\partial}{\partial \mathbf{v}_{\text{P}1}} + \frac{\mathbf{F}_2}{m_{\text{B}}} \frac{\partial}{\partial \mathbf{v}_{\text{P}2}} \right) f_{\text{P}}^{\text{II}}(\mathbf{x}_1, \mathbf{x}_2, \mathbf{v}_{\text{P}1}, \mathbf{v}_{\text{P}2}, t) = \Omega_{\text{PS}}(f_{\text{S}}^{\text{I}}, f_{\text{P}}^{\text{II}}), \quad (25)$$

where \mathbf{F}_1 and \mathbf{F}_2 are the entropic spring forces acting on the beads of the dumbbell. These forces are of the general form $\mathbf{F}_i = (-1)^i H f(\mathbf{Q})$ where $f(\mathbf{Q}) = \mathbf{Q}$ for the Hookean dumbbell, and $f(\mathbf{Q}) = \frac{\mathbf{Q}}{1 - (\mathbf{Q}^2/L_{\text{Qmax}}^2)}$ for a FENE dumbbell where L_{Qmax} represents the maximum extension of the dumbbell. H in these expressions is the spring constant. In the case where the underlying polymer molecule is well represented by a freely jointed bead-rod chain with N beads, connected by rods of length a , one has $H = 3k_{\text{B}}T/[(N-1)a^2]$. In Eq. (25), the self-collision contribution (Ω_{PP}) corresponding to the collisions between beads of different polymers (dumbbells) has been neglected since this contribution is negligibly small in the dilute limit under consideration. Moreover, modeling polymer-polymer interactions in the framework of hard-sphere collisions is not straightforward since instead of bouncing off each other, actual polymer coils tends to interpenetrate one another. These interactions are crucial to account for critical overlap concentration, a parameter of significant importance in semidilute polymeric solutions. A conformation dependent mean-field force, as discussed in Refs. [49–52], can be used to introduce polymer-polymer interactions in the current framework. This force can be modelled alongside the spring force. However, capturing the fluctuations of polymers concentration (phase-separation) in the vicinity of the critical point is more complicated and also requires a nontrivial dependence of osmotic pressure on polymer concentration which can be provided in an *ad hoc* manner in the current framework. The cross-collision term (between solvent molecule and polymer dumbbell) Ω_{PS} is given as

$$\begin{aligned} \Omega_{\text{PS}}(f_{\text{S}}^{\text{I}}, f_{\text{P}}^{\text{II}}) = & \int d\mathbf{v}_{\text{S}} d\mathbf{v}'_{\text{S}1} d\mathbf{v}'_{\text{P}1} [f_{\text{S}}^{\text{I}}(\mathbf{x}_1, \mathbf{v}'_{\text{S}1}, t) f_{\text{P}}^{\text{II}}(\mathbf{x}_1, \mathbf{x}_2, \mathbf{v}'_{\text{P}1}, \mathbf{v}_{\text{P}2}, t) - f_{\text{S}}^{\text{I}}(\mathbf{x}_1, \mathbf{v}_{\text{S}}, t) f_{\text{P}}^{\text{II}}(\mathbf{x}_1, \mathbf{x}_2, \mathbf{v}_{\text{P}1}, \mathbf{v}_{\text{P}2}, t)] \omega_1 \\ & + \int d\mathbf{v}_{\text{S}} d\mathbf{v}'_{\text{S}2} d\mathbf{v}'_{\text{P}2} [f_{\text{S}}^{\text{I}}(\mathbf{x}_2, \mathbf{v}'_{\text{S}2}, t) f_{\text{P}}^{\text{II}}(\mathbf{x}_1, \mathbf{x}_2, \mathbf{v}_{\text{P}1}, \mathbf{v}'_{\text{P}2}, t) - f_{\text{S}}^{\text{I}}(\mathbf{x}_2, \mathbf{v}_{\text{S}}, t) f_{\text{P}}^{\text{II}}(\mathbf{x}_1, \mathbf{x}_2, \mathbf{v}_{\text{P}1}, \mathbf{v}_{\text{P}2}, t)] \omega_2, \end{aligned} \quad (26)$$

where, the first term on the right-hand side accounts for the collision between a solvent molecule and bead 1 located at \mathbf{x}_1 and the second term accounts for the collision between a solvent molecule and bead 2 located at \mathbf{x}_2 . Using the definition of f_{P}^{I} as given in (20) and (25) may again be written in terms of f_{P}^{I} as

$$\begin{aligned} & \left(\frac{\partial}{\partial t} + \mathbf{v}_{\text{P}} \frac{\partial}{\partial \mathbf{x}} \right) f_{\text{P}}^{\text{I}}(\mathbf{x}, \mathbf{v}_{\text{P}}, t) + \frac{1}{m_{\text{B}}} \frac{\partial}{\partial \mathbf{v}_{\text{P}}} \left[\int d\mathbf{x}' d\mathbf{v}'_{\text{P}} \mathbf{F}(\mathbf{x} - \mathbf{x}') [f_{\text{P}}^{\text{II}}(\mathbf{x}, \mathbf{x}', \mathbf{v}_{\text{P}}, \mathbf{v}'_{\text{P}}, t) + f_{\text{P}}^{\text{II}}(\mathbf{x}', \mathbf{x}, \mathbf{v}'_{\text{P}}, \mathbf{v}_{\text{P}}, t)] \right] \\ & = \int d\mathbf{v}_{\text{S}} d\mathbf{v}'_{\text{S}} d\mathbf{v}'_{\text{P}} [f_{\text{S}}^{\text{I}}(\mathbf{x}, \mathbf{v}'_{\text{S}}, t) f_{\text{P}}^{\text{I}}(\mathbf{x}, \mathbf{v}'_{\text{P}}, t) - f_{\text{S}}^{\text{I}}(\mathbf{x}, \mathbf{v}_{\text{S}}, t) f_{\text{P}}^{\text{I}}(\mathbf{x}, \mathbf{v}_{\text{P}}, t)] \omega_1, \end{aligned} \quad (27)$$

which bears a closer resemblance to the kinetic equation (21) for the solvent, but for the obvious change of subscript ($\text{S} \leftrightarrow \text{P}$). The exception is, of course, the entropic force between the beads that still depends on the pair probability density (f_{P}^{II}). It is worth commenting briefly on the timescales

underlying the description based on Eq. (27). There are two such timescales: The first one of $O(m_{\text{B}}/H)^{1/2}$ for the Hookean dumbbell, which characterizes the short-time oscillatory dynamics of the bead under the action of the entropic restoring force, and the second of $O(\zeta/4H)$, ζ being the

friction coefficient, that characterizes the overdamped relaxation of the beads under an instantaneous balance between the entropic spring force and a frictional force. Based on an analogy with the motion of a Brownian particle under the action of a harmonic potential [53], the prevalence of underdamped *vis-à-vis* overdamped dynamics depends on the relative magnitudes of the aforementioned timescales and thus, on the ratio $(m_B H)^{1/2}/\zeta$. The dynamics is overdamped for $(m_B H)^{1/2}/\zeta \ll 1$, which is the limit that is relevant to polymer molecules, and thus, the timescale characterizing the polymeric configuration dynamics is $O(\zeta/4H)$.

A priori it is not obvious that local conservation laws exist in this system. Therefore, in what follows, the set of

conservation laws arising from the kinetic description given by Eq. (21) and Eq. (25) is discussed. Similar to the Boltzmann equation for the simple gas mixture, cross-collisions conserve mass in the present model. Furthermore, as expected, the total momentum is conserved, while individual momenta are not; note that, unlike the binary gas mixture, the natural way to define solute momentum density is by Eq. (15).

On integrating (21) over all possible values of \mathbf{v}_S , the self-collision term goes to zero as before. Using (24) for the cross-collision integral term, and the symmetry of the transition probability with respect to pre- and postcollisional velocities, one gets

$$\begin{aligned} \partial_t \rho_S + \partial_x \cdot \mathbf{J}_S &= m_S \int d\mathbf{v}_S d\mathbf{v}'_{S1} d\mathbf{v}_{P1} d\mathbf{v}'_{P1} f_S^I(\mathbf{x}, \mathbf{v}'_{S1}) f_P^I(\mathbf{x}, \mathbf{v}_{P1}) \omega(\mathbf{v}'_{S1}, \mathbf{v}_{P1} | \mathbf{v}_S, \mathbf{v}_{P1}) \\ &\quad - m_S \int d\mathbf{v}_S d\mathbf{v}'_{S1} d\mathbf{v}_{P1} d\mathbf{v}'_{P1} f_S^I(\mathbf{x}, \mathbf{v}'_{S1}) f_P^I(\mathbf{x}, \mathbf{v}'_{P1}) \omega(\mathbf{v}_S, \mathbf{v}_{P1} | \mathbf{v}'_{S1}, \mathbf{v}'_{P1}) \\ &= 0, \end{aligned} \quad (28)$$

which implies the mass conservation for the solvent. Similarly, the evolution of the solvent momentum density of the solvent is given by

$$\begin{aligned} \partial_t \mathbf{J}_S + \partial_x \cdot \mathbf{P}_S &= m_S \int d\mathbf{v}_S d\mathbf{v}'_{S1} d\mathbf{v}_{P1} d\mathbf{v}'_{P1} \mathbf{v}_S [f_S^I(\mathbf{x}, \mathbf{v}'_{S1}, t) f_P^I(\mathbf{x}, \mathbf{v}'_{P1}, t) - f_S^I(\mathbf{x}, \mathbf{v}_S, t) f_P^I(\mathbf{x}, \mathbf{v}_{P1}, t)] \omega_1 \\ &= m_S \int d\mathbf{v}_S d\mathbf{v}'_{S1} d\mathbf{v}_{P1} d\mathbf{v}'_{P1} [\mathbf{v}_S - \mathbf{v}'_{S1}] f_S^I(\mathbf{x}, \mathbf{v}'_{S1}, t) f_P^I(\mathbf{x}, \mathbf{v}'_{P1}, t) \omega_1, \end{aligned} \quad (29)$$

where \mathbf{P}_S denotes the solvent momentum flux, and similar to the binary gas mixture, the term on the right-hand side of the equation accounts for the momentum exchange between the solvent and polymer components.

Unlike the solvent, showing the existence of mass conservation for the polymer phase is a little more subtle owing to the nonlocality of the dumbbell. The evolution equation for the polymer mass density, defined via Eq. (14), shows the existence of such a conservation law. This evolution equation is written, using Eq. (25), as

$$\partial_t \rho_P + \partial_x \cdot \mathbf{J}_P = m_B \int d\mathbf{x}_2 d\mathbf{v}_{P1} d\mathbf{v}_{P2} \Omega_{PS}(\mathbf{x}_1, \mathbf{x}_2, \mathbf{v}_{P1}, \mathbf{v}_{P2}, t) \delta(\mathbf{x} - \mathbf{x}_1) + m_B \int d\mathbf{x}_1 d\mathbf{v}_{P1} d\mathbf{v}_{P2} \Omega_{PS}(\mathbf{x}_1, \mathbf{x}_2, \mathbf{v}_{P1}, \mathbf{v}_{P2}, t) \delta(\mathbf{x} - \mathbf{x}_2), \quad (30)$$

which, on using symmetry of the transition probability, reduces to the usual continuity equation for the polymer component as

$$\partial_t \rho_P + \partial_x \cdot \mathbf{J}_P = 0, \quad (31)$$

where the momentum density of the polymer phase \mathbf{J}_P has been defined in Eq. (15). The evolution equation for the polymer momentum density takes the form

$$\begin{aligned} \partial_t \mathbf{J}_P + \partial_x \cdot \mathbf{P}_P - \mathbf{I} &= m_B \int d\mathbf{v}_S d\mathbf{v}'_{S1} d\mathbf{v}'_{P1} d\mathbf{v}_{P1} d\mathbf{v}_{P2} d\mathbf{x}_2 \mathbf{v}_{P1} [f_S^I(\mathbf{x}, \mathbf{v}'_{S1}) f_P^{II}(\mathbf{x}, \mathbf{x}_2, \mathbf{v}'_{P1}, \mathbf{v}_{P2}) - f_S^I(\mathbf{x}, \mathbf{v}_S) f_P^{II}(\mathbf{x}, \mathbf{x}_2, \mathbf{v}_{P1}, \mathbf{v}_{P2})] \omega_1 \\ &\quad + m_B \int d\mathbf{v}_S d\mathbf{v}'_{S2} d\mathbf{v}'_{P2} d\mathbf{v}_{P1} d\mathbf{v}_{P2} d\mathbf{x}_1 \mathbf{v}_{P2} [f_S^I(\mathbf{x}, \mathbf{v}'_{S2}) f_P^{II}(\mathbf{x}_1, \mathbf{x}, \mathbf{v}_{P1}, \mathbf{v}'_{P2}) - f_S^I(\mathbf{x}, \mathbf{v}_S) f_P^{II}(\mathbf{x}_1, \mathbf{x}, \mathbf{v}_{P1}, \mathbf{v}_{P2})] \omega_2 \\ &= m_B \int d\mathbf{v}_S d\mathbf{v}'_{S1} d\mathbf{v}_{P1} d\mathbf{v}'_{P1} [\mathbf{v}_P - \mathbf{v}'_{P1}] f_S^I(\mathbf{x}, \mathbf{v}'_{S1}) f_P^I(\mathbf{x}, \mathbf{v}'_{P1}) \omega_1, \end{aligned} \quad (32)$$

where the symmetry of the transition probability has again been used for the collision term. The term \mathbf{I} on the left-hand side of Eq. (32) is defined as

$$\mathbf{I}(\mathbf{x}, t) = \int \mathbf{F}(\mathbf{x}_2 - \mathbf{x}) \psi(\mathbf{x}, \mathbf{x}_2, t) d\mathbf{x}_2 - \int \mathbf{F}(\mathbf{x} - \mathbf{x}_1) \psi(\mathbf{x}_1, \mathbf{x}, t) d\mathbf{x}_1, \quad (33)$$

where the condition $\mathbf{F}_1 = -\mathbf{F}_2 \equiv \mathbf{F}$ is used, with the configuration distribution function ψ being defined as

$$\psi(\mathbf{x}_1, \mathbf{x}_2, t) = \int d\mathbf{v}_1 d\mathbf{v}_2 f_P^{II}(\mathbf{x}_1, \mathbf{x}_2, \mathbf{v}_1, \mathbf{v}_2, t). \quad (34)$$

The local collision of the solvent molecule with individual bead will result in an impulse which is communicated down the backbone of the polymer dumbbell. This motion can also be understood as the nonlocal momentum transfer due to stretching of the polymer spring, the effect of which in polymer momentum density evolution [Eq. (32)] is represented by the term \mathbf{I} .

Coming back to the term, \mathbf{I} , the integral of which over all space is given by

$$\int d\mathbf{x} \mathbf{I}(\mathbf{x}, t) = \int d\mathbf{x} d\mathbf{x}_2 \mathbf{F}(\mathbf{x}_2 - \mathbf{x}) \psi(\mathbf{x}, \mathbf{x}_2, t) - \int d\mathbf{x} d\mathbf{x}_1 \mathbf{F}(\mathbf{x} - \mathbf{x}_1) \psi(\mathbf{x}_1, \mathbf{x}, t) = 0. \quad (35)$$

Thus, global momentum conservation is not affected by \mathbf{I} , and it can, in fact, be defined as the divergence of a second-order tensor as

$$\mathbf{I} = \frac{\partial}{\partial \mathbf{r}} \cdot \boldsymbol{\Theta}. \quad (36)$$

To see this, we note that \mathbf{I} [Eq. (33)] can be rewritten in (\mathbf{r}, \mathbf{Q}) coordinates as

$$\mathbf{I}(\mathbf{r}, t) = \sum_{\nu} \int \mathbf{F}_{\nu}(\mathbf{Q}) \psi(\mathbf{r} - \mathbf{r}_{\nu}, \mathbf{Q}, t) d\mathbf{Q}. \quad (37)$$

Further, assuming the configuration probability density to vary slowly over a dumbbell length, and expanding the configuration distribution function ψ in a Taylor series [47] as

$$\psi(\mathbf{r} - \mathbf{R}_{\nu}, \mathbf{Q}, t) = \psi(\mathbf{r}, \mathbf{Q}, t) - \mathbf{R}_{\nu} \cdot \frac{\partial}{\partial \mathbf{r}} \psi(\mathbf{r}, \mathbf{Q}, t) + \frac{\mathbf{R}_{\nu} \mathbf{R}_{\nu}}{2} : \frac{\partial}{\partial \mathbf{r}} \frac{\partial}{\partial \mathbf{r}} \psi(\mathbf{r}, \mathbf{Q}, t) + \dots, \quad (38)$$

which gives (36) with

$$\boldsymbol{\Theta}(\mathbf{r}, t) = \int \psi(\mathbf{r}, \mathbf{Q}, t) \mathbf{Q} \mathbf{F} d\mathbf{Q}, \quad (39)$$

which is the usual form of the polymeric configurational stress tensor; for Hookean dumbbells, the expression reduces to the spring constant H times the conformation tensor given as $\int \psi(\mathbf{r}, \mathbf{Q}, t) \mathbf{Q} \mathbf{Q} d\mathbf{Q}$. Equation (32) therefore takes the form

$$\partial_t \mathbf{J}_P + \partial_x \cdot \mathbf{P}_P - \partial_x \cdot \boldsymbol{\Theta} = m_B \int d\mathbf{v}_S d\mathbf{v}'_{S1} d\mathbf{v}_{P1} d\mathbf{v}'_{P1} [\mathbf{v}_P - \mathbf{v}'_P] f_S(\mathbf{x}, \mathbf{v}'_{S1}) f_P^I(\mathbf{x}, \mathbf{v}'_{P1}) \omega_1. \quad (40)$$

It should be noted that while the above expansion of the configuration probability density, in yielding the usual elastic stress tensor, is restricted to the characteristic flow dimension being much larger than the polymer radius of gyration, the kinetic theory formulation above is not limited by this assumption. For instance, the term \mathbf{I} , in its original form in Eq. (32), allows for a nonlocal stress tensor in cases where the flow or geometric dimension starts to become comparable to the radius of gyration [54].

Finally, the evolution equation for the total momentum density $\mathbf{J} = \mathbf{J}_P + \mathbf{J}_S$, obtained by adding those for the component momenta [Eqs. (29) and (40)] is

$$\frac{\partial \mathbf{J}}{\partial t} + \frac{\partial}{\partial \mathbf{r}} \cdot (\mathbf{P}_P + \mathbf{P}_S - \boldsymbol{\Theta}) = 0. \quad (41)$$

This conservation form for the total momentum density also implies that the evolution of the momentum densities of the solvent and polymer [Eqs. (21) and (25)] can, similar to the gas mixture, be rewritten in terms of a diffusion velocity as

$$\begin{aligned} \frac{\partial \mathbf{J}_S}{\partial t} + \frac{\partial}{\partial \mathbf{r}} \cdot \mathbf{P}_S(\mathbf{r}, t) &= \frac{1}{\tau_{PS}} \mathbf{V}_D, \\ \frac{\partial \mathbf{J}_P}{\partial t} + \frac{\partial}{\partial \mathbf{r}} \cdot \mathbf{P}_P(\mathbf{r}, t) &= -\frac{1}{\tau_{PS}} \mathbf{V}_D + \frac{\partial}{\partial \mathbf{r}} \cdot \boldsymbol{\Theta}, \end{aligned} \quad (42)$$

where, using Eq. (29), \mathbf{V}_D is defined as

$$\begin{aligned} \mathbf{V}_D &= \tau_{PS} m_S \int d\mathbf{v}_S d\mathbf{v}'_{S1} d\mathbf{v}_{P1} d\mathbf{v}'_{P1} [\mathbf{v}_S - \mathbf{v}'_S] \\ &\quad \times f_S^I(\mathbf{x}, \mathbf{v}'_{S1}, t) f_P^I(\mathbf{x}, \mathbf{v}'_{P1}, t) \omega_1, \end{aligned} \quad (43)$$

$$\begin{aligned} &= -\tau_{PS} m_B \int d\mathbf{v}_S d\mathbf{v}'_{S1} d\mathbf{v}_{P1} d\mathbf{v}'_{P1} [\mathbf{v}_P - \mathbf{v}'_P] \\ &\quad \times f_S^I(\mathbf{x}, \mathbf{v}'_{S1}, t) f_P^I(\mathbf{x}, \mathbf{v}'_{P1}, t) \omega_1. \end{aligned} \quad (44)$$

Here τ_{PS} can again be understood as a timescale associated with the drag force which resists the velocity difference between the two components [24,29].

To conclude, in this section starting from a Boltzmann-like kinetic description of the solvent-polymer mixture in phase space, a set of conservation laws, analogous to those obtained in Refs. [24,27–30], have been obtained for the polymer solution. Indeed, these equations must be reproduced by any model equation written for this system. In subsequent sections, a simple BGK-type model is developed, where these equations are used as consistency conditions.

IV. COLLISION MODEL FOR BINARY GAS MIXTURE

Having introduced the kinetic theory framework for both the binary gas and the polymer-solvent mixtures, we now move on to a brief description of the corresponding collision models for purposes of numerical implementation. As already seen in Sec. II, any self-consistent collision model for the binary gas mixture should obey the following properties:

(1) The self-collision does not affect mass, momentum, and energy conservation:

$$\left\langle \Omega_{jj}, m_j \begin{Bmatrix} 1 \\ \mathbf{v}_j \\ \frac{v_j^2}{2} \end{Bmatrix} \right\rangle = 0. \quad (45)$$

(2) The cross-collision does not affect mass conservation, but leads to momentum and energy exchanges between components such that the total momentum and energy are conserved:

$$\langle m_j \Omega_{jk} \rangle = 0 \text{ with } j \neq k (= A, B), \quad (46)$$

$$\langle \Omega_{AB}, m_A \mathbf{v}_A \rangle + \langle \Omega_{BA}, m_B \mathbf{v}_B \rangle = 0, \quad (47)$$

$$\left\langle \Omega_{AB}, m_A \frac{v_A^2}{2} \right\rangle + \left\langle \Omega_{BA}, m_B \frac{v_B^2}{2} \right\rangle = 0, \quad (48)$$

with $j = A, B$.

(3) Indifferentiability: The mixture description reduces to the single-component description when the components become mechanically equivalent. Thus, when $m_A = m_B$, the total distribution $f = f_A + f_B$ must obey the single species Boltzmann equation [19,48].

(4) Similar to the original Boltzmann equation, the collision model should also have an H theorem of the form

$$\frac{\partial H}{\partial t} + \frac{\partial}{\partial \mathbf{r}} \cdot \mathbf{J}_H = -\sigma, \quad (49)$$

with $\sigma \geq 0$. Here the H function is defined as

$$H = \sum_j^{A,B} \int m_j f_j (\log f_j - 1) d\mathbf{v}, \quad (50)$$

with the flux of H function given by

$$\mathbf{J}_H = \sum_j^{A,B} \int m_j f_j (\log f_j - 1) \mathbf{v}_j d\mathbf{v}_j, \quad (51)$$

and the entropy production being given by

$$\sigma = \sum_j^{A,B} \langle m_j \log f_j, \Omega_j \rangle. \quad (52)$$

Furthermore, the entropy production $\sigma = 0$ if and only if $f_j = f_j^{\text{MB}}(M^{\text{Slow}})$, which implies

$$\Omega_j = 0 \iff f_j = f_j^{\text{MB}}(M^{\text{Slow}}), \quad (53)$$

where f_j^{MB} refers to the local Maxwell-Boltzmann distribution for the j th component, and M^{Slow} refers to the slow manifold comprising the appropriate hydrodynamic variables [12,55].

In what follows, we first describe in brief the BGK and quasiequilibrium approximations for the collision operator, as applied to a binary gas mixture; the following section deals with the quasiequilibrium models for the polymer-solvent mixture. One of the simplest and most widely used models for the collision operator is the single-relaxation time approximation, known as a Bhatnagar-Gross-Krook (BGK)

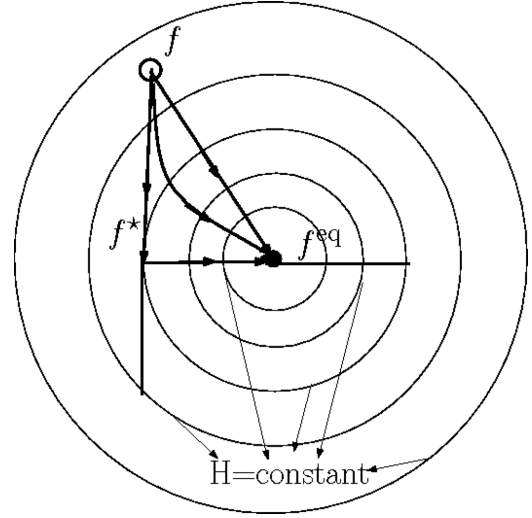


FIG. 6. Scheme showing the relaxation of f to f^{eq} through a quasiequilibrium state f^* .

approximation [56]. Herein, the collision kernel, $\Omega_j = \Omega_{jj} + \Omega_{jk}$, is defined as [48]

$$\Omega_j = \frac{1}{\tau} [f_j^{\text{MB}}(\rho_j, \mathbf{U}, T) - f_j], \quad (54)$$

where $\mathbf{U} = \mathbf{J}/\rho$ is the total mixture velocity and $\rho = \rho_A + \rho_B$ is the mixture mass density. This gives the following form for the rate of change of the nonconserved mixture moments:

$$\begin{aligned} \frac{1}{2} (\langle \Omega_A, m_A \mathbf{v}_A \rangle - \langle \Omega_B, m_B \mathbf{v}_B \rangle) &= -\frac{1}{\tau} \mathbf{V}_D, \\ \sum_j^{A,B} \langle \Omega_j, m_j \mathbf{v}_j \mathbf{v}_j \rangle &= -\frac{1}{\tau} (\mathbf{P} - \mathbf{P}^{\text{eq}}), \end{aligned} \quad (55)$$

where $\mathbf{P}^{\text{eq}} = nk_B T_0 \mathbf{I} + \frac{\mathbf{J}\mathbf{J}}{\rho}$. Equation (55) shows that for the BGK model, the mass diffusion flux and the pressure tensor relax on the same timescale τ , which results in a fixed Schmidt number, Sc (the ratio of the momentum and mass diffusivities) of order unity. One needs at least two different timescales associated with the relaxation rates of the mass diffusion and momentum fluxes, which suggests that the usual BGK collision kernel is not an appropriate model for binary gas mixtures. The single relaxation time approximation is even more inappropriate for polymer-solvent mixtures where due to low center-of-mass diffusivities, polymer mass transfer modes have the extremely long relaxation times, in turn leading to very large values of Sc .

In Refs. [44,45,57] a collision model for binary mixtures, based on an intermediate quasiequilibrium state, has been proposed in order to have a tunable Sc . They followed the concept of a quasiequilibrium as explained in Fig. 6. As shown therein, there is a fast relaxation of the distribution function f towards the quasiequilibrium f^* , followed by a slow relaxation towards the equilibrium state f^{eq} . Both stages of relaxation can be modeled as BGK-type terms with τ_1^{-1} and τ_2^{-1} as the respective rates of relaxation. The equilibrium distribution function f^{eq} is evaluated in the usual manner by minimizing the H function under the constraints of fixed

slow variables M^{Slow} . The quasiequilibrium, f^* , is found by minimizing the H function under the constraints of fixed qasislow variables which, in the present case, can be taken as the individual component momenta [44] or the stresses [57]. The simplest generalization of the BGK model using f^* and the component momenta as quasiconserved variables can be written as

$$\Omega_j = \frac{1}{\tau_1} [f_j^*(\rho_j, \mathbf{u}_j, T_j) - f_j] + \frac{1}{\tau_2} [f_j^{\text{eq}}(\rho_j, \mathbf{U}, T) - f_j^*(\rho_j, \mathbf{u}_j, T_j)]. \quad (56)$$

where the component velocities are defined by $\mathbf{u}_j = \mathbf{J}_j/\rho_j$. It is worth noting that in order to satisfy the H theorem, a proper ordering of the relaxations is required which in the present case corresponds to $\tau_1 \leq \tau_2$ [57,58]. Using the fact $\mathbf{P}^* = \mathbf{P}^{\text{eq}}$, it can be seen that

$$\sum_j^{\text{A,B}} \langle \Omega_j, m_j \mathbf{v}_j \mathbf{v}_j \rangle = -\frac{1}{\tau_1} (\mathbf{P} - \mathbf{P}^{\text{eq}}),$$

$$\frac{1}{2} (\langle \Omega_A, m_A \mathbf{v}_A \rangle - \langle \Omega_B, m_B \mathbf{v}_B \rangle) = -\frac{1}{\tau_2} \mathbf{V}_D, \quad (57)$$

so that the pressure tensor and the diffusion mass flux now relax on different timescales. A Chapman-Enskog expansion shows that the first order nonequilibrium contributions to the pressure tensor \mathbf{P} and the mass diffusion flux \mathbf{V}_D (note that $\mathbf{V}_D^{\text{eq}} = 0$) are [44]

$$\mathbf{P}^{\text{neq}} = \mathbf{P} - \mathbf{P}^{\text{eq}}$$

$$= -\tau_1 n k_B T \left[\left(\frac{\partial \mathbf{U}}{\partial \mathbf{r}} \right) + \left(\frac{\partial \mathbf{U}}{\partial \mathbf{r}} \right)^T - \frac{2\delta}{D} \frac{\partial}{\partial \mathbf{r}} \cdot \mathbf{U} \right],$$

$$\mathbf{V}_D = \tau_2 k_B \left[\frac{\rho_A}{\rho} \frac{\partial (n_B T)}{\partial \mathbf{r}} - \frac{\rho_B}{\rho} \frac{\partial (n_A T)}{\partial \mathbf{r}} \right]. \quad (58)$$

It is evident from Eq. (58) that the shear viscosity μ is proportional to the relaxation time τ_1 as $\mu = n k_B T \tau_1$. Further, and after some rearrangement, the diffusion coefficient D_{AB} can be related to the relaxation time τ_2 giving tunable Sc where $\text{Sc} = \mu/(\rho D_{AB})$. Although tunable, Sc is not arbitrary. The choice of the quasiequilibrium defined by (56), and the implied ordering of the relaxation times, leads to an upper bound on Sc: $\text{Sc} \leq \text{Sc}^*$. The threshold Schmidt number Sc^* depends on the component mass fraction $Y_j(\rho_j/\rho)$ and mole fractions $X_j(n_j/n)$, being given by $\text{Sc}^* = (Y_A Y_B)/(X_A X_B)$; the details of the calculation can be found in [44]. If the component molecular masses, m_j , are of the same order, Sc^* comes out to be the ratio of masses in the dilute limit, and thus use of (56) restricts one to Sc's of order unity or smaller. This is a particularly severe limitation for the polymer-solvent system of interest since, as already mentioned, the small diffusivities of the polymer molecules imply that the typical Schmidt numbers for such systems are very large.

In order to avoid the aforementioned Sc limitation, the elements of the stress tensor \mathbf{P}_j of individual components, can instead be chosen as the set of quasiconserved variables, with the slow variables being the individual mass densities ρ_j and total momentum density $\mathbf{J} = \rho \mathbf{U}$, for purposes of minimizing the H function. Denoting the resulting quasiequilibrium as

$f^{**}(\rho_j, \mathbf{U}, \mathbf{P}_j)$, the collision integral takes the following form:

$$\Omega_j = \frac{1}{\tau_1} [f_j^{**}(\rho_j, \mathbf{U}, \mathbf{P}_j) - f_j] + \frac{1}{\tau_2} [f_j^{\text{eq}}(\rho_j, \mathbf{U}, T) - f_j^{**}(\rho_j, \mathbf{U}, \mathbf{P}_j)]. \quad (59)$$

The nonconserved mixture moments now take the form

$$\sum_j^{\text{A,B}} \langle \Omega_j, m_j \mathbf{v}_j \mathbf{v}_j \rangle = -\frac{1}{\tau_2} \mathbf{P}^{\text{neq}},$$

$$\frac{1}{2} (\langle \Omega_A, m_A \mathbf{v}_A \rangle - \langle \Omega_B, m_B \mathbf{v}_B \rangle) = -\frac{1}{\tau_1} \mathbf{V}_D^{\text{neq}}, \quad (60)$$

and a Chapman-Enskog expansion, similar to the above case, leads to the expressions for the pressure tensor and the mass diffusion flux same as given by Eq. (58) but with the only difference that τ_1 and τ_2 are interchanged. This means that the viscosity μ is now related to τ_2 and the diffusion coefficient D_{AB} to τ_1 . The limitation on Sc is therefore reversed, being given by $\text{Sc} \geq \text{Sc}^*$, which is appropriate to the polymer-solvent mixture. Thus, between them, the two (component momenta and stress-tensor based) quasiequilibria formulations cover the entire range of Sc [44,45,59].

V. COLLISION MODELING FOR POLYMER-SOLVENT MIXTURE

As discussed in Sec. III, the polymer dumbbell collides with the solvent molecule only if the location of the solvent coincides with the location of either of the beads of dumbbell. In order to properly handle the nonlocal polymer-solvent interaction, the required system of kinetic equations are given by

$$\left(\frac{\partial}{\partial t} + \mathbf{v}_S \cdot \frac{\partial}{\partial \mathbf{r}} \right) f_S^I(\mathbf{r}, \mathbf{v}_S, t) = \Omega_S = \Omega_{SS} + \Omega_{SP},$$

$$\left(\frac{\partial}{\partial t} + \mathbf{v}_1 \cdot \frac{\partial}{\partial \mathbf{x}_1} + \mathbf{v}_2 \cdot \frac{\partial}{\partial \mathbf{x}_2} + \frac{\mathbf{F}_1}{m_B} \cdot \frac{\partial}{\partial \mathbf{v}_1} + \frac{\mathbf{F}_2}{m_B} \cdot \frac{\partial}{\partial \mathbf{x}_2} \right) \times f_P^{\text{II}}(\mathbf{x}_1, \mathbf{x}_2, \mathbf{v}_1, \mathbf{v}_2, t) = \Omega_{PS}, \quad (61)$$

where the collision operators Ω_S and Ω_{PS} should be modeled such that the continuum level description, given by (42), is recovered. Similar to the mixture model for the binary gas, one needs two relaxation times in order to have a tunable Sc, and in particular, to be able to access the large Sc's of interest [44,45]. On using the quasiequilibrium-based relaxation method described above, with the component momenta being the quasiconserved variables, the solvent collision term in (61) takes the form

$$\Omega_S = \frac{1}{\tau_1} [f_S^{\text{MB}}(\rho_S, \mathbf{u}_S, T_S) - f_S^I] + \frac{1}{\tau_2} [f_S^{\text{MB}}(\rho_S, \mathbf{U}, T) - f_S^{\text{MB}}(\rho_S, \mathbf{u}_S, T_S)], \quad (62)$$

where $f_S^{\text{MB}}(\rho_S, \mathbf{u}_S, T)$ is the Maxwell-Boltzmann distribution about the solvent velocity \mathbf{u}_S and $f_S^{\text{MB}}(\rho_S, \mathbf{U}, T)$ is the Maxwell-Boltzmann distribution about the solution velocity \mathbf{U} .

The collision term in the polymer kinetic equation (62) must account for the collisions with each of the two beads of the dumbbell; recall that, in (\mathbf{r}, \mathbf{Q}) coordinates, the bead coordinates corresponding to these collisions are $(\mathbf{x}_1, \mathbf{x}_2) \equiv$

$(\mathbf{r}, \mathbf{r} + \mathbf{Q})$ and $(\mathbf{x}_1, \mathbf{x}_2) \equiv (\mathbf{r} - \mathbf{Q}, \mathbf{r})$; the corresponding coordinates for the center of mass and configuration (the dumbbell end-to-end vector) are $(\mathbf{r} + \frac{\mathbf{Q}}{2}, \mathbf{Q})$ and $(\mathbf{r} - \frac{\mathbf{Q}}{2}, \mathbf{Q})$, respectively. Thus, recalling Eq. (26), one may write

$$\Omega_{\text{PS}}(f_S^I, f_P^{\text{II}}) \equiv \Omega_{\text{PS}}^{(1)} \left[f_S^I, f_P^{\text{II}} \left(\mathbf{r} + \frac{\mathbf{Q}}{2}, \mathbf{Q}, \mathbf{v}_P + \frac{\dot{\mathbf{Q}}}{2}, \dot{\mathbf{Q}}, t \right) \right] + \Omega_{\text{PS}}^{(2)} \left[f_S^I, f_P^{\text{II}} \left(\mathbf{r} - \frac{\mathbf{Q}}{2}, \mathbf{Q}, \mathbf{v}_P - \frac{\dot{\mathbf{Q}}}{2}, \dot{\mathbf{Q}}, t \right) \right], \quad (63)$$

where each of the $\Omega_{\text{PS}}^{(v)}$'s are given by a quasiequilibrium ansatz similar to that of the solvent above:

$$\Omega_{\text{PS}}^{(v)} = \frac{1}{\tau_1} [f_P^{\star\text{II}} - f_P^{\text{II}}] + \frac{1}{\tau_2} (f_P^{\text{eqII}} - f_P^{\star\text{II}}), \quad (64)$$

with the arguments of the distributions involved being different for $v = 1$ and 2. Thus, the equilibrium distributions in $\Omega_{\text{PS}}^{(1)}$ and $\Omega_{\text{PS}}^{(2)}$ are

$$\begin{aligned} f_P^{\text{eqII}} \left(\mathbf{r} + \frac{\mathbf{Q}}{2}, \mathbf{Q}, \mathbf{v}_P + \frac{\dot{\mathbf{Q}}}{2}, \dot{\mathbf{Q}} \right) &= \psi \left(\mathbf{r} + \frac{\mathbf{Q}}{2}, \mathbf{Q} \right) \left(\frac{m^{\text{B}}}{2\pi k_{\text{B}} T} \right)^3 \\ &\times \exp \left[- \left(\frac{m^{\text{B}} (\mathbf{v}_P - \mathbf{U}(\mathbf{r}) - \frac{\mathbf{F}_1}{\xi})^2}{2k_{\text{B}} T} \right) - \left(\frac{m^{\text{B}} (\mathbf{v}_P + \dot{\mathbf{Q}} - \mathbf{U}(\mathbf{r} + \mathbf{Q}) - \frac{\mathbf{F}_2}{\xi})^2}{2k_{\text{B}} T} \right) \right], \\ f_P^{\text{eqII}} \left(\mathbf{r} - \frac{\mathbf{Q}}{2}, \mathbf{Q}, \mathbf{v}_P - \frac{\dot{\mathbf{Q}}}{2}, \dot{\mathbf{Q}} \right) &= \psi \left(\mathbf{r} - \frac{\mathbf{Q}}{2}, \mathbf{Q} \right) \left(\frac{m^{\text{B}}}{2\pi k_{\text{B}} T} \right)^3 \\ &\times \exp \left[- \left(\frac{m^{\text{B}} (\mathbf{v}_P - \mathbf{U}(\mathbf{r}) - \frac{\mathbf{F}_2}{\xi})^2}{2k_{\text{B}} T} \right) - \left(\frac{m^{\text{B}} (\mathbf{v}_P - \dot{\mathbf{Q}} - \mathbf{U}(\mathbf{r} - \mathbf{Q}) - \frac{\mathbf{F}_1}{\xi})^2}{2k_{\text{B}} T} \right) \right], \end{aligned} \quad (65)$$

respectively, and the corresponding quasiequilibria are

$$\begin{aligned} f_P^{\star\text{II}} \left(\mathbf{r} + \frac{\mathbf{Q}}{2}, \mathbf{Q}, \mathbf{v}_P + \frac{\dot{\mathbf{Q}}}{2}, \dot{\mathbf{Q}} \right) &= \psi \left(\mathbf{r} + \frac{\mathbf{Q}}{2}, \mathbf{Q} \right) \left(\frac{m^{\text{B}}}{2\pi k_{\text{B}} T} \right)^3 \\ &\times \exp \left[- \left(\frac{m^{\text{B}} [\mathbf{v}_P - \mathbf{u}^r(\mathbf{r} + \frac{\mathbf{Q}}{2})]^2}{2k_{\text{B}} T} \right) - \left(\frac{m^{\text{B}} \{ \mathbf{v}_P + \dot{\mathbf{Q}} - [\mathbf{u}^r(\mathbf{r} + \frac{\mathbf{Q}}{2}) + \mathbf{u}^Q(\mathbf{r} + \frac{\mathbf{Q}}{2})] \}^2}{2k_{\text{B}} T} \right) \right], \\ f_P^{\star\text{II}} \left(\mathbf{r} - \frac{\mathbf{Q}}{2}, \mathbf{Q}, \mathbf{v}_P - \frac{\dot{\mathbf{Q}}}{2}, \dot{\mathbf{Q}} \right) &= \psi \left(\mathbf{r} - \frac{\mathbf{Q}}{2}, \mathbf{Q} \right) \left(\frac{m^{\text{B}}}{2\pi k_{\text{B}} T} \right)^3 \\ &\times \exp \left[- \left(\frac{m^{\text{B}} [\mathbf{v}_P - \mathbf{u}^r(\mathbf{r} - \frac{\mathbf{Q}}{2})]^2}{2k_{\text{B}} T} \right) - \left(\frac{m^{\text{B}} \{ \mathbf{v}_P - \dot{\mathbf{Q}} - [\mathbf{u}^r(\mathbf{r} - \frac{\mathbf{Q}}{2}) - \mathbf{u}^Q(\mathbf{r} - \frac{\mathbf{Q}}{2})] \}^2}{2k_{\text{B}} T} \right) \right]. \end{aligned} \quad (66)$$

Note that the f_P^{eqII} and $f_P^{\star\text{II}}$ are factorized Maxwellians in \mathbf{r} and \mathbf{Q} space with ψ corresponding to the pair probability characterizing the dumbbell configuration. The velocities used in equilibrium distributions [Eq. (65)] comes from the local velocity of the solution, \mathbf{U} as well as due to the contribution of spring force and the corresponding velocities in the quasi equilibrium distribution [Eq. (66)] are the local velocity of the polymer phase given as $\psi \mathbf{u}^r = \int \mathbf{v}_P f_P^{\text{II}} d\mathbf{v}_P d\mathbf{Q}$ and $\psi \mathbf{u}^Q = \int \dot{\mathbf{Q}} f_P^{\text{II}} d\mathbf{v}_P d\mathbf{Q}$. As already discussed, one requirement of the above model is that it should recover the continuum description involving the spatial coordinate (\mathbf{r}) alone, detailed in Sec. III, after integration over the remaining degrees of freedom. A further, stricter, requirement is that the well-known Smoluchowski equation for the configuration distribution function in (\mathbf{r}, \mathbf{Q}) space must be recovered from

the primitive phase-space description, given by (61) and (64), after integration over the velocity degrees of freedom [1]. In order to show that the model does lead to the expected form of the Smoluchowski equation over longer length and timescales, we first define bead-averaged version of any quantity ϕ in configuration space as $\phi(\mathbf{r}, \mathbf{Q}, t) = \sum_v \phi(\mathbf{r} - \mathbf{R}_v, \mathbf{Q}, t)$. Using this definition, we define three lower order moments, the zeroth-order moment $\psi(\mathbf{r}, \mathbf{Q}, t)$, and two first-order moments $\mathbf{J}^r(\mathbf{r}, \mathbf{Q}, t)$ and $\mathbf{J}^Q(\mathbf{r}, \mathbf{Q}, t)$, which are the phase-space averaged momentum density for \mathbf{v}_P and $\dot{\mathbf{Q}}$, respectively. In other words, $\psi = \langle\langle 1 \rangle\rangle$ and $\mathbf{J}^r = \langle\langle \mathbf{v}_P \rangle\rangle$ and $\mathbf{J}^Q = \langle\langle \dot{\mathbf{Q}} \rangle\rangle$ with the operator $\langle\langle \dots \rangle\rangle$ for any arbitrary quantity ϕ being defined as $\langle\langle \phi \rangle\rangle = \sum_v \int d\mathbf{v}_P d\mathbf{Q} \phi f_P^{\text{II}}(\mathbf{r} + \mathbf{R}_v, \mathbf{Q}, \mathbf{v}_P + \dot{\mathbf{Q}}_v, \dot{\mathbf{Q}})$ with \sum_v describing the sum over the contribution of both the beads. The evolution equation of the zeroth (ψ) and two first order

moments (\mathbf{J}^r and \mathbf{J}^Q) takes the following form:

$$\begin{aligned} \frac{\partial}{\partial t} \psi + \frac{\partial}{\partial \mathbf{r}} \cdot \mathbf{J}^r + \frac{\partial}{\partial \mathbf{Q}} \cdot \mathbf{J}^Q &= 0, \\ \frac{\partial}{\partial t} \mathbf{J}^{r,Q} + \frac{\partial}{\partial \mathbf{r}} \cdot \mathbf{P}^{r,rQ} + \frac{\partial}{\partial \mathbf{Q}} \cdot \mathbf{P}^{r,Q,Q} &= \frac{1}{\tau_2} (\mathbf{J}_{\text{eq}}^{r,Q} - \mathbf{J}^{r,Q}), \end{aligned} \quad (67)$$

where the terms \mathbf{P}^r , \mathbf{P}^Q , and \mathbf{P}^{rQ} appearing in the set of equations represented by the second equation (67) are the phase-space averaged second order stress tensors represented as $\langle\langle \mathbf{v}_P \mathbf{v}_P \rangle\rangle$, $\langle\langle \dot{\mathbf{Q}} \dot{\mathbf{Q}} \rangle\rangle$ and $\langle\langle \mathbf{v}_P \dot{\mathbf{Q}} \rangle\rangle$ respectively.

The explicit form of quasiequilibrium distribution function [Eq. (66)] results in $\langle\langle \mathbf{v}_P, \dot{\mathbf{Q}} \rangle\rangle_\star$ to be $\mathbf{J}^{r,Q}$, hence canceling the contribution of first terms of collision operator as represented in Eq. (64). Here the subscript of λ (λ being \star or eq)

on the operator $\langle\langle \dots \rangle\rangle$ defines the distribution function $f^{\lambda \text{II}}$ with respect to which averages are taken. The timescale, τ_2 , is now associated with momentum relaxation process since $\langle\langle \mathbf{v}_P, \dot{\mathbf{Q}} \rangle\rangle_{\text{eq}}$ takes the following form:

$$\begin{aligned} \mathbf{J}_{\text{eq}}^r &= \psi \mathbf{U}(\mathbf{r}, t) + \sum_{\mathbf{v}} \left(\frac{\mathbf{F}_{\mathbf{v}}}{\xi} \psi(\mathbf{r} - \mathbf{R}_{\mathbf{v}}, \mathbf{Q}, t) \right), \\ \mathbf{J}_{\text{eq}}^Q &= \psi(\mathbf{r}, \mathbf{Q}, t) \mathbf{Q} \cdot \frac{\partial \mathbf{U}}{\partial \mathbf{r}} - \psi \frac{2\mathbf{F}}{\xi}. \end{aligned} \quad (68)$$

At this point, it is worth mentioning that a Chapman-Enskog expansion (as detailed in the Appendix), shows that the dynamics at $O(1)$ is the desired Smoluchowski equation which governs the evolution of ψ in conformation ($\mathbf{r} - \mathbf{Q}$) space and is given as

$$\frac{\partial \psi}{\partial t} + \frac{\partial}{\partial \mathbf{r}} \left[\psi \mathbf{U} + \sum_{\mathbf{v}} \left(\frac{\mathbf{F}_{\mathbf{v}}}{\xi} \psi(\mathbf{r} - \mathbf{R}_{\mathbf{v}}, \mathbf{Q}, t) \right) \right] + \frac{\partial}{\partial \mathbf{Q}} \left(\psi \mathbf{Q} \cdot \frac{\partial \mathbf{U}}{\partial \mathbf{r}} - \psi \frac{2\mathbf{F}}{\xi} \right) = \frac{k_B T}{\xi} \left(\frac{\partial^2 \psi}{\partial \mathbf{r}^2} + 2 \frac{\partial^2 \psi}{\partial \mathbf{Q}^2} \right). \quad (69)$$

In the dilute limit, the above equation recovers the desired Smoluchowski equation for the homogeneous case [7,8] and diffusion equation (for the polymer concentration) for the inhomogeneous case [40,41,47] (see the Appendix). By integrating out the conformation degrees of freedom, the polymer mass density ρ_P , the momentum density \mathbf{J}_P , and stress tensor given by Eq. (14), Eq. (15), and Eq. (16), can also be defined in the following manner:

$$\rho_P(\mathbf{r}, t) = \int d\mathbf{Q} m_B \psi(\mathbf{r}, \mathbf{Q}, t), \quad \mathbf{J}_P(\mathbf{r}, t) = \int d\mathbf{Q} m_B \mathbf{J}^r(\mathbf{r}, \mathbf{Q}, t), \quad \mathbf{P}_P(\mathbf{r}, t) = \int d\mathbf{Q} m_B \mathbf{P}^r(\mathbf{r}, \mathbf{Q}, t). \quad (70)$$

Subsequently, Eqs. (67) together with solvent description gives the individual mass conservation represented as

$$\frac{\partial \rho_{(S,P)}}{\partial t} + \frac{\partial \mathbf{J}_{(S,P)}}{\partial \mathbf{r}} = 0, \quad (71)$$

and momentum conservation as

$$\frac{\partial \mathbf{J}_S}{\partial t} + \frac{\partial \mathbf{P}_S}{\partial \mathbf{r}} = \frac{\mathbf{V}_D}{\tau_2}, \quad \frac{\partial \mathbf{J}_P}{\partial t} + \frac{\partial}{\partial \mathbf{r}} (\mathbf{P}_P - \Theta) = -\frac{\mathbf{V}_D}{\tau_2}, \quad (72)$$

where the solvent and polymer phase exchange momentum through the drag term \mathbf{V}_D . It should be emphasized that these are the set of continuum equation which are desired from the present kinetic model [24,27–30]. The drawback of this model is that it will limit the maximum attainable Sc to be equal to mass ratio in the limit of dilute solution [44,57]. In order to avoid this limitation, the relevant collision model is [57]

$$\begin{aligned} \Omega_S &= \frac{1}{\tau_1} [f_S^\star(\rho_S, \mathbf{U}, \mathbf{P}_S) - f_S] + \frac{1}{\tau_2} [f_S^{\text{MB}}(\rho_S, \mathbf{U}) - f_S^\star(\rho_S, \mathbf{U}, \mathbf{P}_S)], \\ \Omega_P &= \frac{1}{\tau_1} [f_P^{\star \text{II}}(\psi, \mathbf{U}, \mathbf{P}^{r,Q,Q}) - f_P^{\text{II}}] + \frac{1}{\tau_2} [f_P^{\text{eq II}}(\psi, \mathbf{U}) - f_P^{\star \text{II}}(\psi, \mathbf{U}, \mathbf{P}^{r,Q,Q})], \end{aligned} \quad (73)$$

such that $\langle f_S^\star, \mathbf{v}_S \mathbf{v}_S \rangle = \mathbf{P}_S$ and $\langle\langle \mathbf{v}_P \mathbf{v}_P, \mathbf{v}_P \dot{\mathbf{Q}}, \dot{\mathbf{Q}} \dot{\mathbf{Q}} \rangle\rangle_\star = \mathbf{P}^{r,Q,Q}$.

This model will give the moment chain the same as Eq. (67) but with the relaxation time τ_1 instead of τ_2 , and therefore the lower limit on Sc will become Sc^\star for the dilute solution, which was the upper limit in the previous model. Physically, the two models differ in terms of the fixed quasivariables. In the first model where Sc^\star is the upper limit, the velocity of individual component is a quasivariable. It means that the system first relaxes to a state with a fixed component velocity and then relaxes to a state which has fixed mass averaged velocity. In the model where Sc^\star is the lower limit, the quasivariable is the pressure tensor of the individual component.

VI. NUMERICAL SCHEME

The lattice Boltzmann scheme is conventionally used as Navier-Stokes equations solver. In the LB formulation, one works with a set of discrete populations $f = \{f_i\}$ which corresponds to predefined discrete velocities \mathbf{c}_i ($i = 1, \dots, N$) to represent the original continuous system [12,60]. In recent years, we have shown that the configurational dynamics of a polymer molecule, that arises from deformation by shear and relaxation by Brownian diffusion, can be effectively recovered when the latter is replaced by a BGK-type relaxation [61,62]. In this section, using a two-dimensional setup, we develop a discrete two fluid kinetic model for polymer solution along the lines of a lattice Boltzmann formulation. The framework

used to represent the solvent and polymer phases is discussed in in Secs. VIA and VIB, respectively.

A. Lattice Boltzmann model for solvent

The solvent phase is represented by probability distribution function f_S (the superscript “I” is removed for simplicity) and the discrete evolution equation of interest is

$$\partial_t f_{Si} + c_{i\alpha} \partial_\alpha f_{Si} = \frac{1}{\tau_1} (f_{Si}^* - f_{Si}) + \frac{1}{\tau_2} (f_{Si}^{\text{eq}} - f_{Si}^*). \quad (74)$$

We choose the D2Q9 model with nine discrete velocities \mathbf{c}_i^S ($i = 0, \dots, 8$) given as

$$\mathbf{c}_i^S = c^S \begin{cases} (0, 0) & \text{if } i = 0 \\ (\cos \frac{(i-1)\pi}{4}, \sin \frac{(i-1)\pi}{4}) & \text{if } i = 1, 2, 3, 4 \\ \sqrt{2} (\cos \frac{(i-1)\pi}{4}, \sin \frac{(i-1)\pi}{4}) & \text{if } i = 5, 6, 7, 8, \end{cases} \quad (75)$$

with the following weights:

$$w_i = \begin{cases} \frac{4}{9} & \text{for } i = 0 \\ \frac{1}{9} & \text{for } i = 1, 2, 3, 4 \\ \frac{1}{36} & \text{for } i = 5, 6, 7, 8. \end{cases} \quad (76)$$

The lattice sound speed c_{SS} is related to the magnitude of discrete velocity c^S as $(c^S)^2 = 3c_{SS}^2$. The macroscopic observables, such as mass density ρ_S , momentum density $\mathbf{J}_S(\rho_S \mathbf{u}_S)$, and stress tensors \mathbf{P}_S are defined as $\sum_i f_{Si} \{1, \mathbf{c}_i^S, \mathbf{c}_i^S \mathbf{c}_i^S\} = \{\rho_S, \mathbf{J}_S, \mathbf{P}_S\}$. The discrete form of the equilibrium distribution function takes the following form [63–65]:

$$f_{Si}^{\text{eq}} = w_i \rho_S \left[1 + \frac{\mathbf{c}_i^S \cdot \mathbf{U}}{c_{SS}^2} + \frac{(\mathbf{c}_i^S \cdot \mathbf{U})^2}{2 c_{SS}^4} - \frac{(\mathbf{U} \cdot \mathbf{U})}{2 c_{SS}^2} \right], \quad (77)$$

an approximate expression that can be improved (by including higher-order terms in U/cs) if needed; recall that \mathbf{U} in Eq. (77) is the total velocity of the solution. Depending on the collision model, the discrete quasiequilibrium distributions take different forms [44,45]. The one where momenta are quasi conserved variables, takes the following form:

$$f_{Si}^* = w_i \rho_S \left[1 + \frac{\mathbf{c}_i^S \cdot \mathbf{u}_S}{c_{SS}^2} + \frac{(\mathbf{c}_i^S \cdot \mathbf{u}_S)^2}{2 c_{SS}^4} - \frac{(\mathbf{u}_S \cdot \mathbf{u}_S)}{2 c_{SS}^2} \right], \quad (78)$$

whereas the one with component stress tensors, as the quasi-conserved variables, takes the form

$$f_{Si}^* = w_i \left[\rho_S + \rho_S \frac{\mathbf{c}_i^S \cdot \mathbf{U}}{c_{SS}^2} + (\mathbf{P}_S - \rho_S c_{SS}^2 \boldsymbol{\delta}) : (\mathbf{c}_i^S \mathbf{c}_i^S - c_{SS}^2 \boldsymbol{\delta}) \right]. \quad (79)$$

Macroscopic quantities pertaining to the mixture, like \mathbf{U} in Eq. (79), may be calculated using the information about the polymer phase, the discrete model of which is described in the subsequent section.

B. Lattice Boltzmann model for polymer

We first recall the distribution function for polymer which does not differentiate between the location of the two beads for the numerical convenience, as

$$f_P(\mathbf{r}, \mathbf{Q}, \mathbf{v}_P, \dot{\mathbf{Q}}, t) = \sum_{\nu} f_P^H(\mathbf{r} - \mathbf{R}_\nu, \mathbf{Q}, \mathbf{v}_P - \dot{\mathbf{R}}_\nu, \dot{\mathbf{Q}}, t). \quad (80)$$

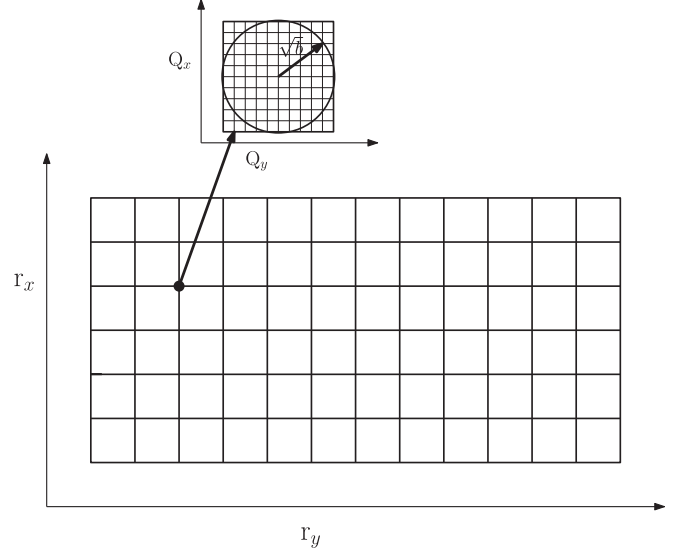


FIG. 7. Four-dimensional configuration space for polymer dumbbell.

For the polymeric solute, to solve a two-dimensional problem in position-orientation space (the orientation being characterized by a single angle), we need to resolve a four-dimensional $\mathbf{r} - \mathbf{Q}$ space as shown in Fig. 7. We chose an unconventional hyperlattice velocity model, the D4Q25 model, to represent the discrete two-particle distribution function of polymer dumbbell in two-dimensional setup. The discrete velocities $(c_{i1}^P, c_{i2}^P, c_{i3}^P, c_{i4}^P) \equiv (v_{ix}, v_{iy}, \dot{Q}_{ix}, \dot{Q}_{iy})$ of the D4Q25 velocity model are given in Table I.

Using the conditions

$$\begin{aligned} \sum_i w_i &= 1, & \sum_i w_i c_{i\alpha}^P c_{i\beta}^P &= c_{\text{SP}}^2 \delta_{\alpha\beta}, \\ \sum_i w_i c_{i\alpha}^P c_{i\beta}^P c_{i\gamma}^P c_{i\delta}^P &= c_{\text{SP}}^2 (\delta_{\alpha\beta} \delta_{\gamma\delta} + \delta_{\alpha\gamma} \delta_{\beta\delta} + \delta_{\alpha\delta} \delta_{\gamma\beta}), \end{aligned} \quad (81)$$

the associated weights can be found as $w_0 = 1/3$ and $w_{1-24} = 1/36$ with $(c^P)^2 = 3c_{\text{SP}}^2$ where c_{SP} is the lattice sound speed for D4Q25 model. The evolution of discrete population is given as

$$\begin{aligned} \left(\frac{\partial}{\partial t} + v_{i\alpha} \frac{\partial}{\partial r_\alpha} + \dot{Q}_{i\alpha} \frac{\partial}{\partial Q_\alpha} \right) f_{Pi}(\mathbf{r}, \mathbf{Q}, \mathbf{v}_P, \dot{\mathbf{Q}}, t) \\ = \frac{1}{\tau_1} (f_{Pi}^* - f_{Pi}) + \frac{1}{\tau_2} (f_{Pi}^{\text{eq}} - f_{Pi}^*). \end{aligned} \quad (82)$$

TABLE I. Discrete velocity set.

r_x	r_y	Q_x	Q_y
0	0	0	0
$\pm c^P$	$\pm c^P$	0	0
$\pm c^P$	0	$\pm c^P$	0
$\pm c^P$	0	0	$\pm c^P$
0	$\pm c^P$	$\pm c^P$	0
0	$\pm c^P$	0	$\pm c^P$
0	0	$\pm c^P$	$\pm c^P$

The moments in conformation ($\mathbf{r} - \mathbf{Q}$) space are defined as $\sum_i f_{Pi} \{1, \mathbf{v}_i, \dot{\mathbf{Q}}, \mathbf{v}_i \mathbf{v}_i, \mathbf{v}_i \dot{\mathbf{Q}}, \dot{\mathbf{Q}} \dot{\mathbf{Q}}\} = \{\psi, \mathbf{J}^r, \mathbf{J}^Q, \mathbf{P}^r, \mathbf{P}^{rQ}, \mathbf{P}^Q\}$. For simplicity, the discrete equilibrium distribution can be expressed up to linear order (as opposed to quadratic order in the solvent case) as

$$f_{Pi}^{\text{eq}} = w_i \left(\psi + \frac{\mathbf{J}^r_{\text{eq}} \cdot \mathbf{v}_i}{c_{sP}^2} + \frac{\mathbf{J}^Q_{\text{eq}} \cdot \dot{\mathbf{Q}}_i}{c_{sP}^2} \right), \quad (83)$$

where the value of \mathbf{J}^r_{eq} and \mathbf{J}^Q_{eq} is given by Eq. (68). The quasiequilibrium distributions take the following form:

$$f_{Pi}^* = w_i \left(\psi + \frac{\mathbf{J}^r \cdot \mathbf{v}_i}{c_{sP}^2} + \frac{\mathbf{J}^Q \cdot \dot{\mathbf{Q}}_i}{c_{sP}^2} \right), \quad (84)$$

for the collision model with competent momenta as quasi-conserved variable, whereas the one with component stress tensors, as the quasiconserved variables, takes the form

$$f_{Pi}^* = w_i \left[\psi + \frac{\mathbf{J}^r_{\text{eq}} \cdot \mathbf{v}_i}{c_{sP}^2} + \frac{\mathbf{J}^Q_{\text{eq}} \cdot \dot{\mathbf{Q}}_i}{c_{sP}^2} + (\mathbf{P}^r - \psi c_{sP}^2 \delta) : (\mathbf{v}_i \mathbf{v}_i - c_{sP}^2 \delta) + \mathbf{P}^{rQ} : (\mathbf{v}_i \dot{\mathbf{Q}}_i) + (\mathbf{P}^Q - \psi c_{sP}^2 \delta) : (\dot{\mathbf{Q}}_i \dot{\mathbf{Q}}_i - c_{sP}^2 \delta) \right]. \quad (85)$$

C. Time discretization

This section reviews the time discretization scheme. In the lattice Boltzman scheme, Eqs. (74) and (82) are discretized in time by applying the implicit trapezoidal rule between time t as

$$\begin{aligned} f_{ji}(\mathbf{x} + \mathbf{c} \Delta t, t + \Delta t) &= f_{ji}(\mathbf{x}, t) + \frac{\Delta t}{2} \{ \Omega_j [f_{ji}(\mathbf{x}, t)] + \Omega_j \\ &\times [f_{ji}(\mathbf{x} + \mathbf{c}^j \Delta t, t + \Delta t)] \}, \end{aligned} \quad (86)$$

where $j = S, P$ and $\Omega_{S,P}$ represents the collision operator for solvent or polymer [11]. In order to make the method explicit, following auxiliary function, g_{ji} , is introduced which depends on original distribution function, f_{ji} , as

$$g_{ji} = f_{ji} - \frac{\Delta t}{2} \left[\frac{1}{\tau_1} (f_{ji} - f_{ji}^*) + \frac{1}{\tau_2} (f_{ji}^* - f_{ji}^{\text{eq}}) \right]. \quad (87)$$

After the transformation, the resultant discrete equation becomes

$$\begin{aligned} g_{ji}(\mathbf{x} + \mathbf{c}^j \Delta t, t + \Delta t) &= g_{ji}(\mathbf{x}, t) (1 - 2\beta) + 2\beta \left[\left(1 - \frac{\tau_1}{\tau_2} \right) f_{ji}^* + \frac{\tau_1}{\tau_2} f_{ji}^{\text{eq}} \right], \end{aligned} \quad (88)$$

where $\beta = \Delta t / (2\tau_1 + \Delta t)$. Since, g_{ji} depends on the both f_{ji}^* and f_{ji}^{eq} , the collision model require the evaluation of the moments of in term of f_{ji} . Therefore,

$$\begin{aligned} \rho_S(f_S) &= \rho_S(g_S), \quad \psi(f_P) = \psi(g_P); \\ \mathbf{J}_S(f_S) &= \frac{\frac{2\tau_{1,2}}{\Delta t} \mathbf{J}_S(g_S) + \rho_S \mathbf{U}}{1 + \frac{2\tau_{1,2}}{\Delta t}}, \quad \mathbf{J}_r(f_P) = \frac{\frac{2\tau_{1,2}}{\Delta t} \mathbf{J}_r(g_P) + \mathbf{J}_{\text{eq}}^r}{1 + \frac{2\tau_{1,2}}{\Delta t}}. \end{aligned} \quad (89)$$

It is worth mentioning at this point that in order to calculate polymeric contribution to the total velocity, \mathbf{U} , we need to further integrate out the conformation dependence of polymer momentum density. Therefore, the dependence of the transformation into the auxiliary function, \mathbf{g} , on total moments looks like $\rho(f) = \rho(g)$ and

$$\mathbf{U}(f) = \mathbf{U}(g) + (\Delta t / 2\tau_{1,2}) \Theta(g) / \rho. \quad (90)$$

Finally, the initial condition on $\psi(\mathbf{r}, \mathbf{Q}, t)$ at every location in \mathbf{r} is given as

$$\psi(\mathbf{r}, \mathbf{Q}, 0) = \begin{cases} N_{\text{eq}} (1 - Q^2/b)^{b/2} & \text{for } |Q| \leq \sqrt{b} \\ 0 & \text{elsewhere,} \end{cases} \quad (91)$$

where $N_{\text{eq}} = 2\pi b^{3/2} B[3/2, (b+2)/2]$ and $B\{x, y\}$ is the Beta function. The FENE spring force has a singularity at $Q = \sqrt{b}$ for limiting the maximum extension of the spring up to a length of \sqrt{b} . The simulation domain in Q space is limited inside a circle of radius \sqrt{b} as shown in Fig. 7. The bounce-back boundary condition is applied at the boundaries of the circle [11,12,66].

VII. VISCOELASTIC KOLMOGOROV FLOW

In this section, we validate the kinetic theory formulation detailed in the earlier sections by showing that the presented model is capable of capturing the viscoelastic effects exhibited by polymer solutions. We choose the Kolmogorov flow for this purpose. In this flow, a unidirectional body force varying sinusoidally in space, and represented as $\mathbf{f} = [F \cos(y/l), 0]$, is used to induce a parallel flow with velocity $U \cos(y/l)$. The magnitude of the force is given as $F = \eta U / l^2$, with η being the viscosity.

The Newtonian Kolmogorov flow becomes linearly unstable for Reynolds number (Re) greater than $\sqrt{2}$ [67], the essentially inviscid instability arising from the presence of inflection points in the base-state sinusoidal velocity profile. For the case of a dilute polymer solution, effects of elasticity have been shown to stabilize the Newtonian inflectional instability associated with a shear layer [68]. The stabilization arises because the stretched polymers lead to the perturbed shear layer acting as a deformed elastic membrane, and the resulting restoring force leads to the damping of short-wavelength perturbations (see the Appendix by Hinch in [68]). Subsequent efforts [69–73] have examined the susceptibility of Kolmogorov flow, and other wall-bounded unidirectional shearing flows, to elastoinertial instabilities. Very recently, elasticity alone has been shown to destabilize a unidirectional shearing flow [74], even in the absence of inertia. The mechanism underlying the aforementioned elastoinertial and purely elastic instabilities is currently under examination, and the subsequent nonlinear evolution is therefore beyond the scope of the present numerical investigation.

For purposes of numerically verifying the stabilizing action of elasticity on Kolmogorov flow, we consider a unit cell in two-dimensional physical space, of side 2π , discretized using 72 grid points. We use 32 grid points to discretize the conformation space. Periodic boundary conditions are used in both spatial directions for the solvent as well as the polymer solver. A Gaussian random field is used to seed the instability

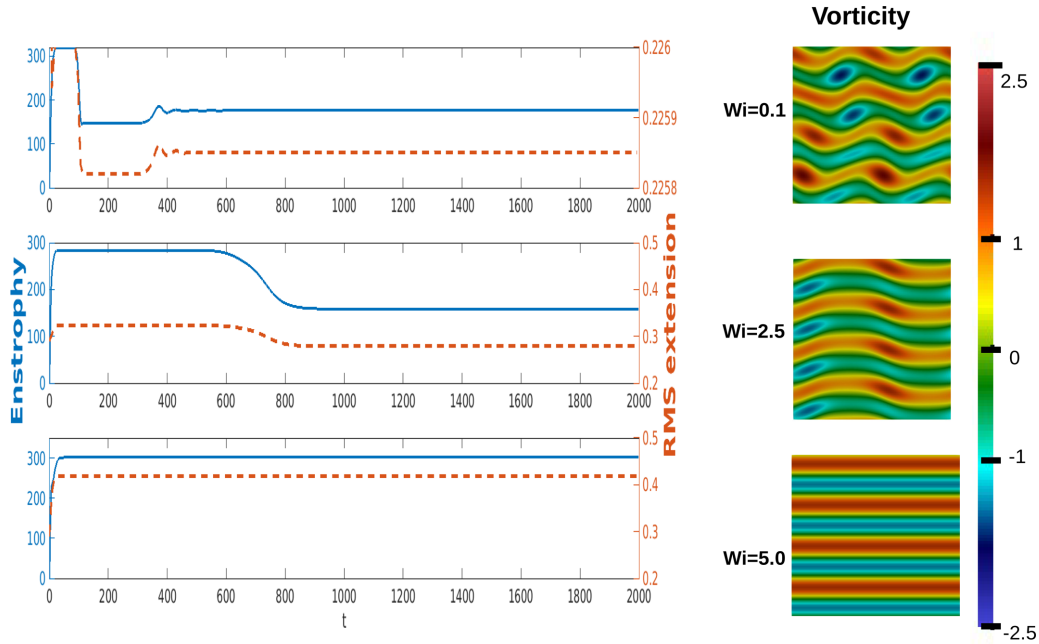


FIG. 8. Time dynamics of the enstrophy, the rms polymer extension, and the corresponding vorticity fields at time $t = 2000$, convection time units at $\text{Re} = 3.5$, and $\beta = 0.5$ with varying Wi .

in the flow. In our study, we use $l = 1/4$, implying that the unit cell incorporates four periods of the Kolmogorov profile. The Reynolds number, Re , is defined using the kinematic viscosity of solution, ν , as Ul/ν . The additional physical parameters needed for the viscoelastic case are as follows. The first parameter is β which represents the ratio of the solvent viscosity η_s to the solution viscosity ($\eta_s + \eta_p$), with the polymeric contribution to the viscosity $\eta_p = n_p k_B T \tau_R$; here n_p is the polymer number density and the timescale $\tau_R (= \zeta/4H)$ characterizes the restoring action of the spring force. Next, we have the Weissenberg number defined as $\text{Wi} = U\tau_R/l$. Finally, for the FENE dumbbells used to represent the polymer molecules, there also arises the maximum extensibility parameter b . For our calculations, b is set to be 25; for choices of the other parameters used, the value of Sc lies between 0.05 and 4.0. To explore the effect of polymer-induced elasticity, we consider a scenario where the flow is unstable to infinitesimal amplitude perturbations in the Newtonian limit; accordingly, $\text{Re} = 3.5$.

Figure 8 shows the vorticity fields ($\boldsymbol{\omega} = \nabla \times \mathbf{u}$ with \mathbf{u} being the flow velocity) characterizing the saturated nonlinear state, and the temporal development of global quantities—both the enstrophy (defined as $1/2 \int (\boldsymbol{\omega} \cdot \boldsymbol{\omega}) dx dy$) and the root-mean-square extension of the polymer [defined as $Q_{\text{rms}}(\mathbf{x}, \mathbf{y}, t) = \sqrt{\langle \psi Q^2 \rangle / \langle \psi \rangle}$, where ψ is the conformation probability density and can be understood as the zeroth moment of the pair-probability distribution characterizing the polymer molecule, that is, $\psi = \sum_i f_{Pi}$]. The temporal development of the enstrophy may be explained as follows. On short timescales, momentum diffusion arising from the induced forcing leads to the laminar sinusoidal velocity profile for all three Wi examined. For the two smaller Wi 's, there is a decrease in the enstrophy on longer timescales, corresponding to the onset of the inflectional instability mentioned

above. The onset of instability, and the associated velocity fluctuations at the chosen Re lead to a higher rate of viscous dissipation, in turn leading to a mean profile that is still nearly sinusoidal but with a smaller amplitude. This smaller amplitude leads to a lower enstrophy and is responsible for the aforementioned decrease in enstrophy. Note that this decrease happens on a shorter timescale for $\text{Wi} = 0.1$ owing to the instability having a nearly Newtonian character. For $\text{Wi} = 2.5$, the decrease is delayed, and has a marginally smaller magnitude, reflecting an elasticity-induced stabilization. The corresponding vorticity field plot shows that the saturated state for $\text{Wi} = 2.5$ is characterized by a larger length scale in the streamwise direction; this increase in the characteristic length scale is consistent with the tendency of the stresses arising from stretched polymers acting to damp out the shorter wavelength perturbations arising from an inflectional instability [68]. On increasing Wi to 5, the instability disappears, which is likely due to the dominant unstable modes shifting to wavelengths that are larger than the size of the periodic domain; correspondingly, the enstrophy remains at the plateau value, corresponding to the laminar profile, for all time. The plots of the root-mean-square polymer extension field reflect the trends in the enstrophy variation mentioned above.

In order to understand what actually happens due to the nonhomogeneity of flow on polymer, we first consider the case for $\text{Wi} = 0.1$. For this low Wi , the polymer feedback to the flow will be minimal. Figures 9(a)–9(c) show, respectively the scenario just before and after the instability and for much longer times corresponding to the nonlinear saturated state. To orient the reader, in Fig. 9(a) we have also plotted the sinusoidal forcing over four periods, used to initiate the Kolmogorov flow. Before instability onset, at $t = 70$, the figure shows the expected one-dimensional variations of the norm of velocity gradient (defined as $|\partial_y u_x + \partial_x u_y|$) and

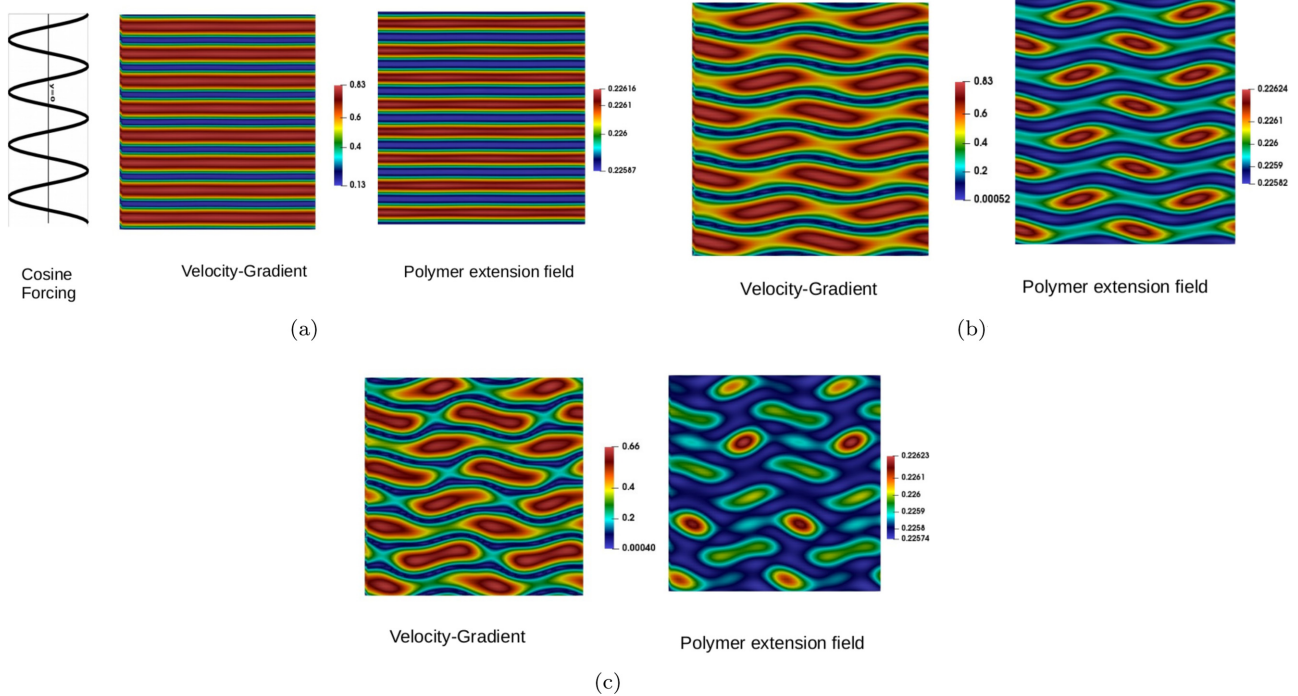


FIG. 9. Spatial distribution of global quantities (the norm of the fluid velocity gradient and the rms-polymer extension field), for $Re = 3.5$ and $Wi = 0.1$, at three different time instants corresponding to before and just after instability onset, and corresponding to the long-time saturated state. (a) $t = 70$ (b) 90 (c) Saturated state ($t = 2000$).

polymer extension fields, with the greatest extensions correlating to the maximum values of the velocity gradient. At $t = 97$, when the inflectional instability has just developed, one starts to observe the emergence of two-dimensional variations in the aforementioned fields in Fig. 9(b). Finally, the saturated two-dimensional fields are shown in Fig. 9(c), corresponding to $t = 2000$. For the small Wi chosen, one notes the modest of Q_{rms} which fluctuates around 0.2 which is the equilibrium extension value, l_0 for the chosen parameter b (i.e., $1/\sqrt{25}$); the polymer concentration field remains virtually homogeneous for all times.

Similar to the previous case, for $Wi = 2.5$, we again considered three time instances: Just before and after the instability and at a long time corresponding to the nonlinear saturated state in Fig. 10. At $t = 400$, Fig. 10(a) shows that the flow remain in the unidirectional laminar state, with both the velocity gradient and the polymer extension exhibiting a one-dimensional variation. As expected, the peak values associated with the polymer extension are higher than those corresponding to the earlier figure with $Wi = 0.1$ (see Fig. 8). In Fig. 10(b), corresponding to $t = 700$, a time considerably longer than that for $Wi = 0.1$, there are signatures associated with the onset of an instability owing to the appearance of a long-wavelength modulation of the original base-state contours of both the velocity gradient and polymer extension. Figure 10(c) shows that the saturated instability in the velocity gradient, as mentioned earlier, is now characterized by a larger length scale in the streamwise direction and the polymer extension is now fully concentrated in the extremum of flow gradient. For $Wi = 5$ (not shown), the polymers completely suppress the original inertial instability, as already mentioned, and as a result, the velocity gradient and polymer extension

fields remain similar to the base laminar state as shown in either Fig. 9(a) or Fig. 10(a); the only difference being that Q_{rms} now attains a higher value (close to 0.5), nearly twice that for $Wi = 0.1$.

VIII. CONCLUSION

We have presented a kinetic-level coupling of polymer-solvent system in phase space using a Boltzmann-type formulation for binary mixtures. Unlike binary gas mixtures of simple molecules, one encounters an asymmetry in the description of the individual components. This happens because the polymer molecule, as modeled by a dumbbell, is represented by a two-particle distribution function, whereas the solvent phase molecule is represented by a single-particle distribution function. The detailed kinetic scheme also results in a continuum picture where dissipative coupling between the two phases (an *ad hoc* assumption in earlier efforts) occurs naturally. The present kinetic formulation leads to the Smoluchowski equation governing the configurational dynamics of the polymer molecules. Using this kinetic description, a numerical algorithm is then built along the lines of the usual lattice Boltzmann technique. Finally, via numerical simulation of two-dimensional viscoelastic Kolmogorov flow, we are able to recover one of the principal effects of suspended polymers on an ambient shearing flow: That of the suppression of inflectional instabilities due to inertia, in turn leading to a saturated nonlinear state characterized by a length scale that increases with increasing Wi . In the presence scheme, the polymer-solvent coupling occurs in velocity space via the equilibrium distribution that involves a contribution from the spring force. There is no restriction on the

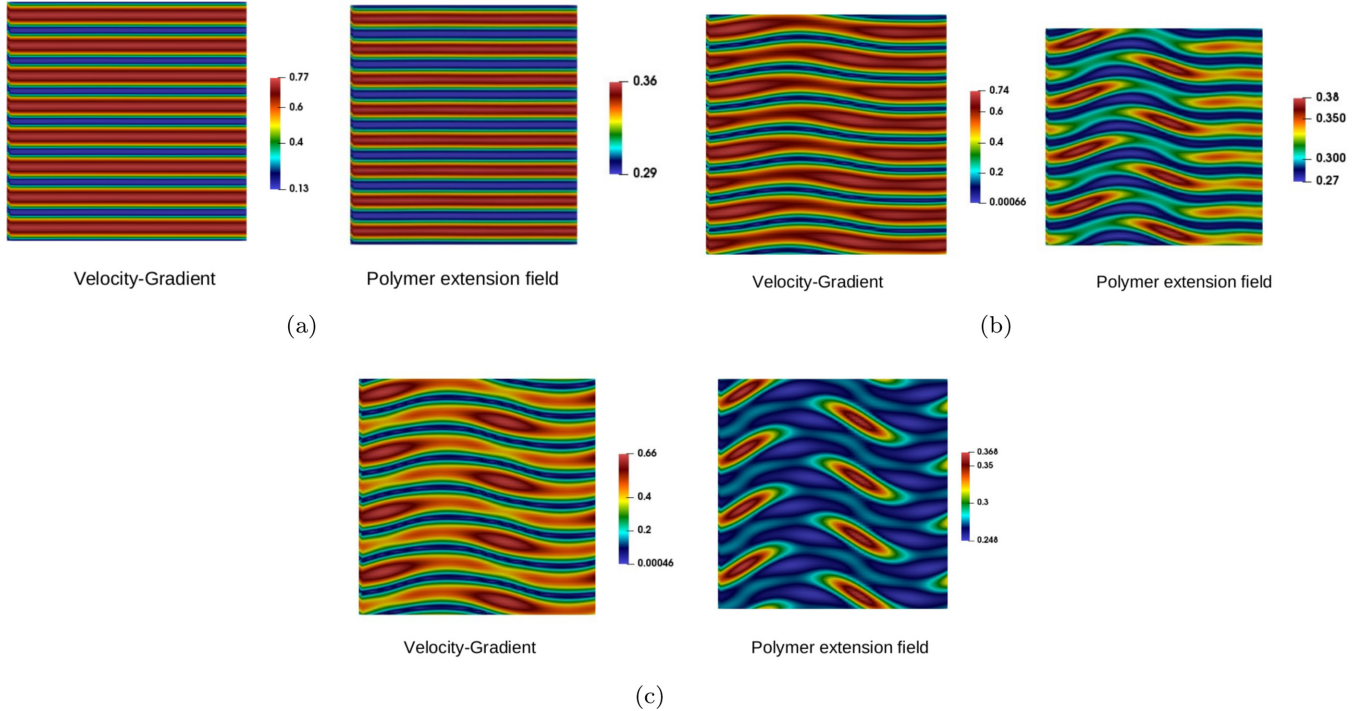


FIG. 10. Spatial distribution of global quantities at $Re = 3.5$ and $Wi = 2.5$ at different time. (a) $t = 400$ (b) $t = 700$ (c) Saturated state ($t = 2000$).

form of the spring force that is used, thereby eliminating the need of any closure approximations. Therefore, this scheme has the potential to advance our understanding of viscoelastic flow phenomena, including instabilities, particularly in cases where the polymer molecules are represented by realistic micromechanical models, going beyond the Hookean dumbbell/bead-spring representations.

Finally, it is worth commenting on the computation expense involved. The current scheme explores the dynamics in the configuration-cum-position space of of polymer molecule. As a result, there is an additional overhead in terms of memory requirement. If the system size of the presented flow is extended to three dimensions with 72 grid points in real space and 32 grid points in configuration (Q -) space, the realistic memory requirement is estimated around 5–7 TB. A typical computing cluster of 32 nodes, (assuming 24 cores per node) and assuming memory of 8 GB per core, will have around 6.0 TB RAM. Thus, due to intrinsic parallel nature of current algorithm such simulations are quite feasible. This coupling scheme is expected performs extremely well for lower dimension polymer models like dumbbell for a wide range of Wi as compared to its stochastic counterpart [75]. However, the RAM requirement dramatically increases with the increase in number of bead for N -bead polymer model. Furthermore, for

problems where conformation fluctuations do play a crucial role, for instance, in the translocation of DNA molecules through nanopores [76], the current LB framework can be generalized to a fluctuating one along the lines represented by Adhikari *et al.* [77], however, with an increase in computation time.

ACKNOWLEDGMENTS

S.S. acknowledges the financial support by EPSRC (UK) Grant No. (EP/N016602/1) and the Leverhulme Early Career Fellowship (ECF-2019-100). S.A. thanks SERB funding for the project “Multiscale Modeling of Complex Fluids.” S.S. acknowledges the use of the Scientific Computing Research Technology Platform and associated support services at the University of Warwick, in the completion of this work. S.S. also acknowledges the support of the International Institute of Carbon-Neutral Energy Research (I2CNER), Japan, during the intermediate developmental phase of the computational scheme. S.S. would like to thank James Sprittles and Laura Cooper (University of Warwick, Coventry, UK) and Takeshi Tsuji (I2CNER, Kyushu University; currently at the University of Tokyo) for helpful discussions related to this work.

APPENDIX: CHAPMAN-ENSKOG EXPANSION

In this Appendix, using a multiscale Chapman-Enskog expansion, it is shown that in the present BGK-type collision model [Eq. (64)], the correct slow dynamics of configuration distribution function is recovered in the dilute limit for both the homogeneous as well as inhomogeneous case. In the Chapman-Enskog multiscale expansion, f_p^{II} is expanded as

$$f_p^{\text{II}} = f_p^{\text{eqII}} + \tau f_p^{(1)\text{II}} + \tau^2 f_p^{(2)\text{II}} + \dots \quad \text{such that} \quad \int f^{(n)\text{II}} d\mathbf{Q} d\mathbf{v} = 0 \quad \text{for} \quad n > 1. \quad (\text{A1})$$

The consequence of this is that the nonconserved moments can also be expanded in powers of smallest timescale τ ($\tau_{1,2}$ depending on collision model) around their equilibrium values. For example, the momentum and the second-order moments, $\mathbf{M}(\mathbf{J}^r, \mathbf{J}^Q, \mathbf{P}^r, \mathbf{P}^{rQ}, \mathbf{P}^Q)$ have the following expansions:

$$\mathbf{M} = \mathbf{M}^{\text{req}} + \tau \mathbf{M} + \dots, \quad (\text{A2})$$

where the leading order contribution to equilibrium values are

$$\begin{aligned} \mathbf{J}^{\text{req}} &= \psi(\mathbf{r}, \mathbf{Q}, t) \mathbf{U} + \sum_{\nu} \left(\frac{\mathbf{F}_{\nu}}{\zeta} \psi(\mathbf{r} - \mathbf{R}_{\nu}, \mathbf{Q}, t) \right), & \mathbf{J}^{\text{Qeq}} &= \psi(\mathbf{r}, \mathbf{Q}, t) \mathbf{Q} \cdot \frac{\partial \mathbf{U}}{\partial \mathbf{r}} - \psi(\mathbf{r}, \mathbf{Q}, t) \frac{2\mathbf{F}}{\zeta}, \\ \mathbf{P}^{\text{req}} &= \psi(\mathbf{r}, \mathbf{Q}, t) \frac{k_{\text{B}} T}{m_{\text{B}}} \delta, & \mathbf{P}^{\text{rQeq}} &= \sum_{\nu} (-1)^{\nu} \psi(\mathbf{r} - \mathbf{R}_{\nu}, \mathbf{Q}, t) \delta, & \mathbf{P}^{\text{Qeq}} &= 2\psi(\mathbf{r}, \mathbf{Q}, t) \frac{k_{\text{B}} T}{m_{\text{B}}} \delta. \end{aligned} \quad (\text{A3})$$

The time derivative is also expanded as

$$\frac{\partial \phi}{\partial t} = \frac{\partial^{(0)} \phi}{\partial t} + \tau \frac{\partial^{(1)} \phi}{\partial t} + \dots. \quad (\text{A4})$$

The moment equation (67) at the zeroth order is

$$\begin{aligned} -\mathbf{J}^{r(1)} &= \left[\frac{\partial}{\partial \mathbf{r}} \cdot \left(\psi(\mathbf{r}, \mathbf{Q}, t) \frac{k_{\text{B}} T}{m_{\text{B}}} \delta \right) + \frac{\partial}{\partial \mathbf{Q}} \mathbf{P}^{\text{rQeq}} \right] + \frac{\partial^{(0)}}{\partial t} \mathbf{J}^{\text{req}}, \\ -\mathbf{J}^{\text{Q}(1)} &= \left[\frac{\partial}{\partial \mathbf{r}} \cdot \mathbf{P}^{\text{rQeq}} + \frac{\partial}{\partial \mathbf{Q}} \cdot \left(2\psi(\mathbf{r}, \mathbf{Q}, t) \frac{k_{\text{B}} T}{m_{\text{B}}} \delta \right) \right] + \frac{\partial^{(0)}}{\partial t} \mathbf{J}^{\text{Qeq}}, \end{aligned} \quad (\text{A5})$$

which gives the configuration distribution evolution as

$$\begin{aligned} \frac{\partial}{\partial t} \psi(\mathbf{r}, \mathbf{Q}, t) + \frac{\partial}{\partial \mathbf{r}} \left[\psi(\mathbf{r}, \mathbf{Q}, t) \mathbf{U} + \sum_{\nu} \left(\frac{\mathbf{F}_{\nu}}{\zeta} \psi(\mathbf{r} - \mathbf{R}_{\nu}, \mathbf{Q}, t) \right) \right] + \frac{\partial}{\partial \mathbf{Q}} \left(\psi(\mathbf{r}, \mathbf{Q}, t) \mathbf{Q} \cdot \frac{\partial \mathbf{U}}{\partial \mathbf{r}} - \psi(\mathbf{r}, \mathbf{Q}, t) \frac{2\mathbf{F}}{\zeta} \right) \\ = \frac{k_{\text{B}} T}{\zeta} \left(\frac{\partial^2 \psi}{\partial \mathbf{r}^2} + 2 \frac{\partial^2 \psi}{\partial \mathbf{Q}^2} \right), \end{aligned} \quad (\text{A6})$$

where τ is characteristic timescale for velocity fluctuations defined as $\tau = m_{\text{B}}/\zeta$ [47,78].

1. Homogeneous flow in dilute limit

In the dilute limit $\mathbf{U}(\mathbf{r}, t) \approx \mathbf{u}_{\text{S}}(\mathbf{r}, t)$ and for homogeneous flows the elements of velocity gradient tensor $\nabla \mathbf{u}_{\text{S}}$ can be taken as constant. Therefore on integrating the \mathbf{r} degrees of freedom from Eq. (A6), one gets

$$\frac{\partial}{\partial t} \psi(\mathbf{Q}, t) + \frac{\partial}{\partial \mathbf{Q}} \cdot \left(\psi(\mathbf{Q}, t) \mathbf{Q} \cdot \frac{\partial \mathbf{u}_{\text{S}}}{\partial \mathbf{r}} - \psi(\mathbf{r}, \mathbf{Q}, t) \frac{2\mathbf{F}}{\zeta} + \frac{2k_{\text{B}} T}{\zeta} \frac{\partial \psi}{\partial \mathbf{Q}} \right) = 0, \quad (\text{A7})$$

which is the desired Smoluchowski equation in the homogeneous flow scenario.

2. Density diffusion equation in dilute limit

In order to obtain the polymer density equation, \mathbf{Q} degrees are integrated out from Eq. (A6), which gives

$$\frac{\partial}{\partial t} \rho_{\text{P}}(\mathbf{r}, t) + \frac{\partial}{\partial \mathbf{r}} \cdot \left(\rho_{\text{P}} \mathbf{U} + \frac{m_{\text{B}}}{\zeta} \frac{\partial}{\partial \mathbf{r}} \Theta_{\alpha\beta} + \frac{m_{\text{B}}^2}{\zeta} \int d\mathbf{Q} J_{\alpha}^{\text{r}(1)} \right) = 0, \quad (\text{A8})$$

after multiplying with m_{B} . The last term of the above equation is given as

$$-m_{\text{B}} \int d\mathbf{Q} J_{\alpha}^{\text{r}(1)} = \left[\frac{\partial}{\partial r_{\beta}} \left(\rho_{\text{P}}(\mathbf{r}, t) \frac{k_{\text{B}} T}{m_{\text{B}}} \delta_{\alpha\beta} \right) \right] + \frac{\partial^{(0)}}{\partial t} (\rho_{\text{P}}(\mathbf{r}, t) U_{\alpha}). \quad (\text{A9})$$

Using the total momentum conservation at the macroscopic level,

$$\frac{\partial \mathbf{J}}{\partial t} + \frac{\partial}{\partial \mathbf{r}} \cdot \mathbf{P}(\mathbf{r}, t) = \frac{\partial}{\partial \mathbf{r}} \cdot \Theta, \quad (\text{A10})$$

we get

$$-\frac{m_{\text{B}}^2}{\zeta} \int d\mathbf{Q} J_{\alpha}^{\text{r}(1)} = \frac{\partial}{\partial r_{\beta}} \left(\rho_{\text{P}}(\mathbf{r}, t) \frac{k_{\text{B}} T}{\zeta} \delta_{\alpha\beta} \right) + \underbrace{\frac{\rho_{\text{P}}}{\rho} \frac{\partial}{\partial r_{\beta}} \left(\frac{m_{\text{B}}}{\zeta \tau_{1,2}} \Theta_{\alpha\beta} - n k_{\text{B}} T \delta_{\alpha\beta} \right)}_{\Xi}. \quad (\text{A11})$$

In the dilute limit $\rho_P/\rho \rightarrow 0$, therefore the term $\Xi \rightarrow 0$. In terms of number density ($\rho_P = 2n_P m_B$), we get

$$\frac{\partial}{\partial t} n_P(\mathbf{r}, t) + \frac{\partial}{\partial r_\alpha} \left(n_P U_\alpha + \frac{1}{2\zeta} \frac{\partial}{\partial r_\beta} \Theta_{\alpha\beta} \right) = \frac{k_B T}{\zeta} \frac{\partial^2 n_P}{\partial r^2}, \quad (\text{A12})$$

which is the required density equation [40,41,47].

-
- [1] R. B. Bird, C. F. Curtiss, R. C. Armstrong, and O. Hassager, *Dynamics of Polymeric Liquids* (Wiley, New York, 1987), Vol. 1-2.
- [2] R. G. Larson, *Constitutive Equations for Polymer Melts and Solutions* (Butterworths, 1988).
- [3] H. A. Castillo Sánchez, M. R. Jovanović, S. Kumar, A. Morozov, V. Shankar, G. Subramanian, and H. J. Wilson, Understanding viscoelastic flow instabilities: Oldroyd-B and beyond, *J. Non-Newtonian Fluid Mech.* **302**, 104742 (2022).
- [4] R. Keunings, On the Peterlin approximation for finitely extensible dumbbells, *J. Non-Newtonian Fluid Mech.* **68**, 85 (1997).
- [5] G. Lielens, P. Halin, I. Jaumain, R. Keunings, and V. Legat, New closure approximations for the kinetic theory of finitely extensible dumbbells, *J. Non-Newtonian Fluid Mech.* **76**, 249 (1998).
- [6] G. Lielens, R. Keunings, and V. Legat, The FENE-L and FENE-LS closure approximations to the kinetic theory of finitely extensible dumbbells, *J. Non-Newtonian Fluid Mech.* **87**, 179 (1999).
- [7] M. Laso and H. C. Öttinger, Calculation of viscoelastic flow using molecular models: The connfessit approach, *J. Non-Newtonian Fluid Mech.* **47**, 1 (1993).
- [8] K. Feigl, M. Laso, and H. C. Öttinger, CONNFESSIT approach for solving a two-dimensional viscoelastic fluid problem, *Macromolecules* **28**, 3261 (1995).
- [9] H. C. Öttinger, *Stochastic Processes in Polymeric Fluids: Tools and Examples for Developing Simulation Algorithms* (Springer, New York, 1996).
- [10] M. A. Hulsen, A. P. G. Van Heel, and B. H. A. A. Van Den Brule, Simulation of viscoelastic flows using Brownian configuration fields, *J. Non-Newtonian Fluid Mech.* **70**, 79 (1997).
- [11] S. Chen and G. D. Doolen, Lattice Boltzmann method for fluid flows, *Annu. Rev. Fluid Mech.* **30**, 329 (1998).
- [12] S. Succi, *The Lattice Boltzmann Method for Fluid Dynamics and Beyond* (Oxford University Press, New York, 2001).
- [13] C. K. Aidun and J. R. Clausen, Lattice-Boltzmann method for complex flows, *Annu. Rev. Fluid Mech.* **42**, 439 (2010).
- [14] P. Ahrlichs and B. Dünweg, Lattice-Boltzmann simulation of polymer-solvent systems, *Int. J. Mod. Phys. C* **9**, 1429 (1998).
- [15] R. M. Jendrejack, D. C. Schwartz, J. J. De Pablo, and M. D. Graham, Shear-induced migration in flowing polymer solutions: Simulation of long-chain DNA in microchannels, *J. Chem. Phys.* **120**, 2513 (2004).
- [16] T. T. Pham, U. D. Schiller, J. R. Prakash, and B. Dünweg, Implicit and explicit solvent models for the simulation of a single polymer chain in solution: Lattice Boltzmann versus Brownian dynamics, *J. Chem. Phys.* **131**, 164114 (2009).
- [17] P. Ahrlichs and B. Dünweg, Simulation of a single polymer chain in solution by combining lattice Boltzmann and molecular dynamics, *J. Chem. Phys.* **111**, 8225 (1999).
- [18] A. Jain, P. Sunthar, B. Duenweg, and J. R. Prakash, Optimization of a Brownian-dynamics algorithm for semidilute polymer solutions, *Phys. Rev. E* **85**, 066703 (2012).
- [19] L. Sirovich, Kinetic modeling of gas mixtures, *Phys. Fluids* **5**, 908 (1962).
- [20] E. Goldman and L. Sirovich, Equations for gas mixtures, *Phys. Fluids* **10**, 1928 (2004).
- [21] Y. Onishi, H. Chen, and A. Ohashi, A lattice Boltzmann model for polymeric liquids, *Prog. Comp. Fluid Dyn.* **5**, 75 (2005).
- [22] O. Malaspinas, N. Fietier, and M. Deville, Lattice Boltzmann method for the simulation of viscoelastic fluid flows, *J. Non-Newtonian Fluid Mech.* **165**, 1637 (2010).
- [23] A. Gupta, M. Sbragaglia, and A. Scagliarini, Hybrid lattice Boltzmann/finite difference simulations of viscoelastic multi-component flows in confined geometries, *J. Comput. Phys.* **291**, 177 (2015).
- [24] S. T. Milner, Hydrodynamics of Semidilute Polymer Solutions, *Phys. Rev. Lett.* **66**, 1477 (1991).
- [25] C. Rangel-Nafaile, A. B. Metzner, and K. F. Wissbrun, Enhanced concentration fluctuations in polymer solutions under shear flow, *Macromolecules* **17**, 1187 (1984).
- [26] X. L. Wu, D. J. Pine, and P. K. Dixon, Enhanced Concentration Fluctuations in Polymer Solutions Under Shear Flow, *Phys. Rev. Lett.* **66**, 2408 (1991).
- [27] E. Helfand and G. H. Fredrickson, Large Fluctuations in Polymer Solutions Under Shear, *Phys. Rev. Lett.* **62**, 2468 (1989).
- [28] M. Doi and A. Onuki, Dynamic coupling between stress and composition in polymer solutions and blends, *J. Phys. II* **2**, 1631 (1992).
- [29] S. T. Milner, Dynamical theory of concentration fluctuations in polymer solutions under shear, *Phys. Rev. E* **48**, 3674 (1993).
- [30] H. Ji and E. Helfand, Concentration fluctuations in sheared polymer solutions, *Macromolecules* **28**, 3869 (1995).
- [31] M. Cromer, M. C. Villet, G. H. Fredrickson, and L. G. Leal, Shear banding in polymer solutions, *Phys. Fluids* **25**, 051703 (2013).
- [32] P. D. Olmsted, Perspectives on shear banding in complex fluids, *Rheol. Acta* **47**, 283 (2008).
- [33] M. D. Graham, Fluid dynamics of dissolved polymer molecules in confined geometries, *Annu. Rev. Fluid Mech.* **43**, 273 (2011).
- [34] P. O. Brunn, The effect of a solid wall for the flow of dilute macromolecular solutions, *Rheol. Acta* **15**, 23 (1976).
- [35] P. O. Brunn, Wall effects in simple shear of dilute polymer solution: Exact results for very narrow and very wide channels, *J. Non-Newtonian Fluid Mech.* **24**, 343 (1987).

- [36] H. Ma and M. D. Graham, Theory of shear-induced migration in dilute polymer solutions near solid boundaries, *Phys. Fluids* **17**, 083103 (2005).
- [37] R. M. Jendrejack, D. C. Dimalanta, E. T. Schwartz, M. D. Graham, and J. J. de Pablo, DNA Dynamics in a Microchannel, *Phys. Rev. Lett.* **91**, 038102 (2003).
- [38] A. V. Bhave, R. C. Armstrong, and R. A. Brown, Kinetic theory and rheology of dilute, nonhomogeneous polymer solutions, *J. Chem. Phys.* **95**, 2988 (1991).
- [39] P. O. Brunn, Non-uniform concentration profiles of dilute macromolecular solutions in rotational viscometric flows, *J. Chem. Phys.* **80**, 3420 (1984).
- [40] A. N. Beris and V. G. Mavrantzas, On the compatibility between various macroscopic formalisms for the concentration and flow of dilute polymer solutions, *J. Rheol.* **38**, 1235 (1994).
- [41] M. V. Apostolakis, V. G. Mavrantzas, and A. N. Beris, Stress gradient-induced migration effects in the Taylor-Couette flow of a dilute polymer solution, *J. Non-Newtonian Fluid Mech.* **102**, 409 (2002).
- [42] M. D. Chilcott and J. M. Rallison, Creeping flow of dilute polymer solutions past cylinders and spheres, *J. Non-Newtonian Fluid Mech.* **29**, 381 (1988).
- [43] J. M. Rallison and E. J. Hinch, Do we understand the physics in the constitutive equation?, *J. Non-Newtonian Fluid Mech.* **29**, 37 (1988).
- [44] S. Arcidiacono, J. Mantzaras, S. Ansumali, I. V. Karlin, C. Frouzakis, and K. B. Boulouchos, Simulation of binary mixtures with the lattice Boltzmann method, *Phys. Rev. E* **74**, 056707 (2006).
- [45] S. Arcidiacono, I. V. Karlin, J. Mantzaras, and C. Frouzakis, Lattice Boltzmann model for the simulation of multicomponent mixtures, *Phys. Rev. E* **76**, 046703 (2007).
- [46] S. Chapman and T. G. Cowling, *The Mathematical Theory of Non-Uniform Gases: An Account of the Kinetic Theory of Viscosity, Thermal Conduction, and Diffusion in Gases* (Cambridge University Press, 1991).
- [47] H. C. Öttinger and F. Petrillo, Kinetic theory and transport phenomena for a dumbbell model under nonisothermal conditions, *J. Rheol.* **40**, 857 (1996).
- [48] P. Andries, K. Aoki, and B. Perthame, A consistent BGK-type model for gas mixtures, *J. Stat. Phys.* **106**, 993 (2002).
- [49] R. C.-Y. Ng and L. G. Leal, Concentration effects on birefringence and flow modification of semidilute polymer solutions in extensional flows, *J. Rheol.* **37**, 443 (1993).
- [50] R. C.-Y. Ng and L. G. Leal, A study of the interacting fene dumbbell model for semi-dilute polymer solutions in extensional flows, *Rheol. Acta* **32**, 25 (1993).
- [51] C. Schneggenburger, M. Kröger, and S. Hess, An extended FENE dumbbell theory for concentration dependent shear-induced anisotropy in dilute polymer solutions, *J. Non-Newtonian Fluid Mech.* **62**, 235 (1996).
- [52] S. Chaffin and J. Rees, Semi-dilute dumbbells: Solutions of the Fokker-Planck equation, *J* **4**, 341 (2021).
- [53] U. M. Titulaer, A systematic solution procedure for the Fokker-Planck equation of a Brownian particle in the high-friction case, *Physica A* **91**, 321 (1978).
- [54] P. O. Brunn and S. Grisafi, Kinetic theory of a dilute polymer solution in a small channel: Equilibrium results, *Chem. Eng. Commun.* **36**, 367 (1985).
- [55] C. Cercignani, *The Boltzmann Equation* (Springer, 1988).
- [56] P. L. Bhatnagar, E. P. Gross, and M. Krook, A model for collision processes in gases. I. Small amplitude processes in charged and neutral one-component systems, *Phys. Rev.* **94**, 511 (1954).
- [57] S. Ansumali, S. Arcidiacono, S. S. Chikatamarla, N. I. Prasianakis, A. N. Gorban, and I. V. Karlin, Quasi-equilibrium lattice Boltzmann method, *Eur. Phys. J. B* **56**, 135 (2007).
- [58] A. N. Gorban and I. V. Karlin, General approach to constructing models of the Boltzmann equation, *Physica A* **206**, 401 (1994).
- [59] S. Arcidiacono, S. Ansumali, I. V. Karlin, J. Mantzaras, and K. B. Boulouchos, Entropic lattice Boltzmann method for simulation of binary mixtures, *Math. Comput. Sim.* **72**, 79 (2006).
- [60] R. Benzi, S. Succi, and M. Vergassola, The lattice Boltzmann equation: Theory and applications, *Phys. Rep.* **222**, 145 (1992).
- [61] S. Singh, G. Subramanian, and S. Ansumali, A lattice Boltzmann method for dilute polymer solutions, *Philos. Trans. R. Soc. A* **369**, 2301 (2011).
- [62] S. Singh, G. Subramanian, and S. Ansumali, Lattice Fokker Planck for dilute polymer dynamics, *Phys. Rev. E* **88**, 013301 (2013).
- [63] Y. H. Qian, D. d’Humières, and P. Lallemand, Lattice BGK models for Navier-Stokes equation, *Europhys. Lett.* **17**, 479 (1992).
- [64] X. Shan and X. He, Discretization of the Velocity Space in the Solution of the Boltzmann Equation, *Phys. Rev. Lett.* **80**, 65 (1998).
- [65] F. J. Higuera, S. Succi, and R. Benzi, Lattice gas dynamics with enhanced collisions, *Europhys. Lett.* **9**, 345 (1989).
- [66] A. J. C. Ladd, Numerical simulations of particulate suspensions via a discretized Boltzmann equation. Part 2. Numerical results, *J. Fluid Mech.* **271**, 311 (1994).
- [67] L. D. Meshalkin and I. G. Sinai, Investigation of the stability of a stationary solution of a system of equations for the plane movement of an incompressible viscous liquid, *J. Appl. Math. Mech.* **25**, 1700 (1961).
- [68] J. Azaiez and G. M. Homsy, Linear stability of free shear flow of viscoelastic liquids, *J. Fluid Mech.* **268**, 37 (1994).
- [69] G. Boffetta, A. Celani, A. Mazzino, A. Puliafito, and M. Vergassola, The viscoelastic Kolmogorov flow: Eddy viscosity and linear stability, *J. Fluid Mech.* **523**, 161 (2005).
- [70] S. Berti, A. Bistagnino, G. Boffetta, A. Celani, and S. Musacchio, Two-dimensional elastic turbulence, *Phys. Rev. E* **77**, 055306(R) (2008).
- [71] P. Garg, I. Chaudhary, M. Khalid, V. Shankar, and G. Subramanian, Viscoelastic Pipe Flow Is Linearly Unstable, *Phys. Rev. Lett.* **121**, 024502 (2018).
- [72] M. Khalid, I. Chaudhary, P. Garg, V. Shankar, and G. Subramanian, The centre-mode instability of viscoelastic plane Poiseuille flow, *J. Fluid Mech.* **915**, A43 (2021).
- [73] Y. Dubief, J. Page, R. R. Kerswell, V. E. Terrapon, and V. Steinberg, A first coherent structure in elasto-inertial turbulence, *Phys. Rev. Fluids* **7**, 073301 (2022).
- [74] M. Khalid, V. Shankar, and G. Subramanian, Continuous Pathway between the Elasto-Inertial and Elastic Turbulent States in Viscoelastic Channel Flow, *Phys. Rev. Lett.* **127**, 134502 (2021).
- [75] M. Melchior and H. C. Öttinger, Variance reduced simulations of polymer dynamics, *J. Chem. Phys.* **105**, 3316 (1996).

- [76] B. Lu, F. Albertorio, D. P. Hoogerheide, and J. A. Golovchenko, Origins and consequences of velocity fluctuations during DNA passage through a nanopore, *Biophys. J.* **101**, 70 (2011).
- [77] R. Adhikari, K. Stratford, M. E. Cates, and A. J. Wagner, Fluctuating lattice Boltzmann, *Europhys. Lett.* **71**, 473 (2005).
- [78] J. D. Schieber and H. C. Öttinger, The effects of bead inertia on the Rouse model, *J. Chem. Phys.* **89**, 6972 (1988).